INVESTIGATING GRAYWATER FILTRATION EFFICACY OF PACIFIC NORTHWEST PUMICE AND SCORIA

by

MARGERY BRIGHT PRICE

A THESIS

Presented to the Department of Earth Sciences
and the Robert D. Clark Honors College
in partial fulfillment of the requirements for the degree of
Bachelor of Science

May 2022

An Abstract of the Thesis of

Margery Price for the degree of Bachelor of Science
in the Department of Earth Sciences to be taken June 2022

Title: Investigating Graywater Filtration Efficacy of Pacific Northwest Pumice and Scoria

Approved: *Thomas Giachetti, Ph.D.*
Primary Thesis Advisor

Graywater is non-sewage wastewater from washing machines, bathing, and cleaning. It can be recycled if particles of shampoo, soap, and other contaminants can be removed, usually by filtration through a medium such as gravel or sand. Such graywater recycling methods are becoming increasingly important as water crises worsen worldwide and fresh water becomes scarcer. This project aims at testing the potential of pumice and scoria (porous volcanic rocks) from Oregon volcanoes as efficient filters for graywater recycling. After characterizing the physical properties of the rock samples (size, shape, porosity), we carried out week-long experiments in which graywater interacts with different size fractions of the two types of rock to identify the best graywater filter. We find that, among the samples tested, 1-2-mm pumice particles are the most effective filtration media amongst those tested. Immersion of graywater in these samples results in the neutralization of the graywater pH to a value of 6.8 and a >75% decrease in turbidity after seven days. The interaction of the rock particles with the graywater also leads to an increase in Total Dissolved Solids (TDS). More work needs to be done analyzing the complex chemical and physical interactions between the rocks and the graywater.

Acknowledgements

To my advisor, Dr. Thomas Giachetti, thank you immensely for your guidance in this research. I am incredibly lucky to be part of this wonderful, exciting, meaningful project. To my second reader, Dr. Matthew Polizzotto, and to my CHC faculty representative, Dr. Samantha Hopkins, thank you for your patience and enthusiasm throughout this arduous process. To Pat Heins, Kory Russel, Kurt Langworthy, Markus Koeneke, Erin Drumm (OSU), and everyone else who so generously contributed information during my research process, thank you for your willingness to collaborate with and help me. To my colleagues and professors in the Department of Earth Sciences and the Clark Honors College, thank you for being part of the enriching, supportive, and uplifting academic communities that have brought me so much growth and joy. To my friends and family, thank you for every moment of encouragement and aid. I am grateful for all of you beyond words.

In the completion of this project and degree, I received financial assistance from the University of Oregon, the College of Arts and Sciences, the Clark Honors College, the Department of Earth Sciences, the Lincoln City Rotary and Kiwanis clubs, the Williams Family, and many other generous donors. This project specifically was made possible by funding from the UO Incubating Interdisciplinary Initiatives (I3) award and from the UO Presidential Undergraduate Research Scholarship program.

Table of Contents

List of Figures

List of Tables

Background and Project Introduction

This senior thesis project characterizes pumice and scoria from central Oregon and monitors static immersion of samples in tap water and graywater. My research aims at identifying key characteristics of these volcanic rocks which influence their efficacy as filtration media. The project lays a foundation for future work exploring flow mechanics in active-flow graywater filtration systems with these or similar volcanic samples. This research was conducted in 2021 and 2022 under the supervision of Dr. Thomas Giachetti in the University of Oregon Department of Earth Sciences. Underlined words can be found in the Glossary section.

Background

Graywater and graywater filtration

Graywater is gently-used wastewater expelled from washing machines, showers, tubs, and sinks. Depending on its source (such as industrial or domestic), graywater may contain a wide variety of particles, both chemical (such as drain cleaner, shampoo, and laundry detergent) and physical (such as toothpaste, hair, and food particles) (Abedin, et al., 2013). It is distinct from blackwater, which contains fecal matter, although in some municipal wastewater treatment systems, the two are managed together. Statistics on graywater use and production are limited in the United States, due both to strict regulations regarding wastewater treatment and to a lack of robust graywater research in the country (Pat Heins, Oregon DEQ, personal comm.). As described in depth in the Literature Review, however, many sources exist which have analyzed graywater production in regions such as Africa and the Middle East; Abedin, et al. (2013),

analyzing graywater in Dhaka City (Bangladesh), found that graywater composed up to 70% of household wastewater in their area of study.

Individual household graywater systems have only been permitted by the state government of Oregon since 2011. In the eleven years since the permit system opened, only 53 domestic graywater reuse systems have been implemented in the state, more than 40 of which are simple laundry systems, in which untreated or minimally treated laundry water is piped to an outdoor irrigation network. It is estimated that there are many more unregulated systems in the state that are not in compliance with or officially registered with the state (Pat Heins, Oregon DEQ, personal communication).

Processes to clean and reuse graywater have been an area of active study in the field of wastewater recycling for several decades. Many systems have been created that use unfiltered graywater for water needs not reliant on drinking-quality water, such as graywater from laundry machines irrigating tomato plants (Misra et al., 2010). In modern industrial, municipal, domestic, and agricultural systems, there are many tasks for which fresh, potable water is used. These include landscape and crop irrigation, cooling of machinery and vehicles, washing of streets and buildings, and more. Utilizing recycled graywater for these functions instead of fresh, potable water, decreases societal consumption of the latter, thus extending the longevity of water resources for current and future generations.

As governments and economies across the globe struggle with environmental change, population increase, and resource conflicts, methods to conserve fresh water are crucial. Prominent water shortages and droughts are already occurring from California to South Africa, heightened by increasing societal demands for water. Ongoing

urbanization and industrialization concentrate both water needs and water pollution, further straining water infrastructure. To maintain a sustainable and stable societal future, it is necessary to improve the world's water systems, including facilitating more efficient and widespread wastewater treatment and recycling programs.

To clean graywater, the chemical and physical constituents added in homes and other buildings (e.g., soap, deodorant, dust, grease) must be removed. This removal typically involves filtration, in which graywater flows through a medium in or on which particles get trapped or absorbed, effectively removing them from the water. Multiple types of filtration systems exist, including those that use screens or mesh, vegetation, and sediment. Sediment filters, also referred to as bed filters, usually consist of a horizontal container filled with sediment (from clay to sand to gravel in size), through which water is channeled in a horizontal direction (see Figure 1). During flow, particles in the water interact with and adhere to the outside of the filtration media, and so the water leaving the system is cleaner than when it entered. Thus, in bed filters, filtration materials with higher surface area are more efficient, since they can interact more with the water and thus potentially retain more particles.

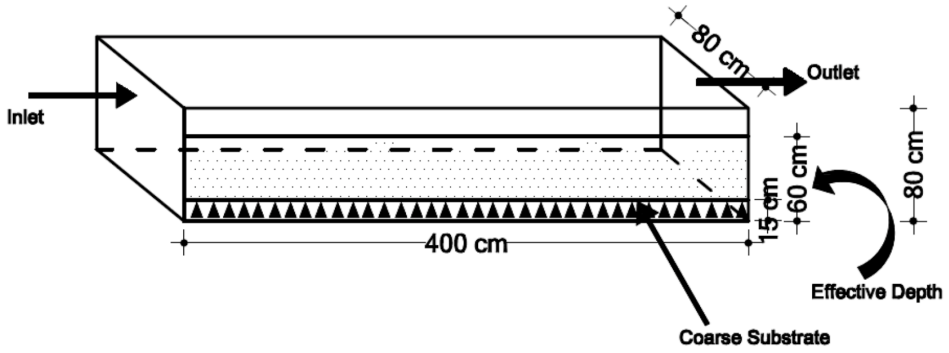

Figure 1: Bed filter diagram from Aregu, et al. (2021)

Pumice and scoria

Because of the importance of the surface area in filter materials, pumice and scoria are being closely studied as potential candidate media in bed filtration systems. Each is a type of highly porous rock formed and ejected during volcanic eruptions. Pumice is felsic, usually pale in color and often so porous it can float on water, whereas scoria is commonly denser, more mafic, and ranges from dark red to brown in color. Both are used in varieties of industrial and societal capacities–pumice used frequently as an abrasive (both domestically, in personal or household cleaning products, and industrially, as a material to soften stiff fabrics such as denim) and scoria used in landscaping and road support. The two pyroclasts form in different environments: pumice in explosive eruptions of viscous magmas rich in silica (SiO_2); scoria usually in more effusive eruptions of less-viscous lava with lower silica content.

In both eruptive settings, the presence of gas in the magma creates vesicles (i.e., bubbles) that exist as void space in the rock, contributing to the rocks' porous nature. Most of these vesicles are connected to the outside surface of the rock, although some, especially in pumices, are isolated and do not reach the outside– see Figure 2. Pumices and scoriae are very porous as they are volumetrically mainly composed of vesicles,

with their solid material consisting of glass forming the walls surrounding vesicles or and crystals. Typically, pumice has very high porosity, with the porosity of some samples reaching 90% but most between 60-90%; scoria has lower but still fairly high porosity, typically around 50-80% (Mueller, et al., 2011).

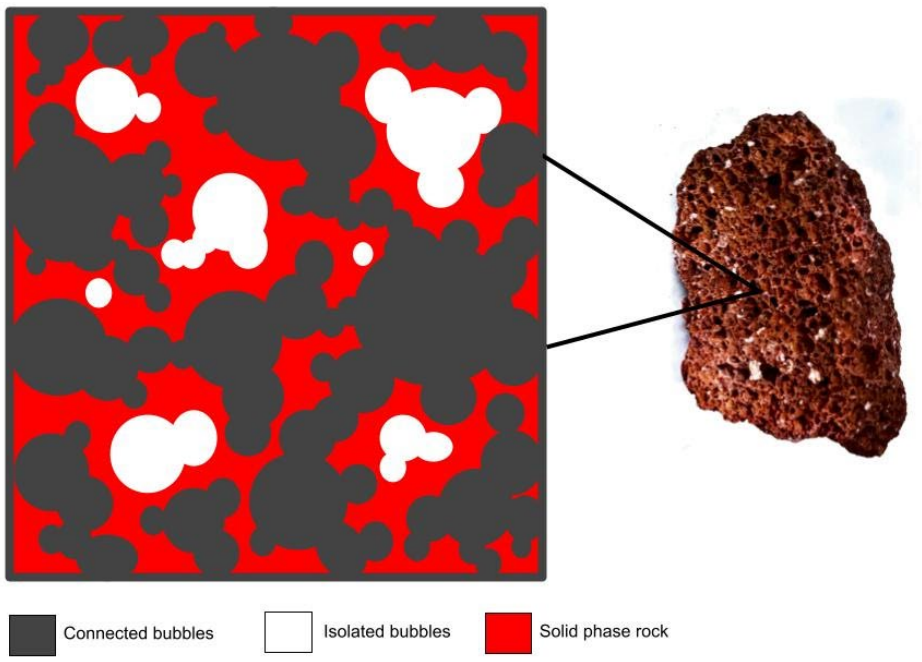

Figure 2. Schematic diagram illustrating the different types of porosities (connected and isolated) within individual particles

Connected pores (dark), also called “open pores,” are void spaces which connect to the environment outside the particle. Isolated pores (white), also called “closed pores,” are bubbles of gas which are surrounded by solid phase rock (red) and do not connect to the outside.

Pumice and scoria as graywater filtration media

It is their high porosity that makes pumice and scoria ideal candidates for being filtration media. A bed filter composed of pumices or scoriae contains not only the

surface area of the outside of each clast, but also the surface area formed by the internal, yet interconnected, bubble network, increasing the amount of surface area available to capture particles from flowing water. When water flows through the bed, it is possible that its molecules may move in and out of the pore space, interacting with the bubble interior walls in addition to with the exterior surface area. This means that bed filters with higher-porosity materials can theoretically conduct more filtration than bed filters with identically-sized but non-porous filtration materials (e.g., sand).

In considering the worldwide need for water recycling systems, pumice and scoria are ideal candidates for graywater filter media for another reason: their ubiquity. These rocks are created in wide ranges of eruptive settings around the world and are some of the most frequent products of volcanoes. They are generated en masse and have been for millions of years; deposits of pyroclasts can stretch hundreds of meters in thickness and contain several tons of material. Eight hundred million people around the globe live in or near volcanic regions (see Figure 3), such as in Andean South America, Indonesia, Japan, East Africa, New Zealand, the U.S. Pacific Northwest, and Iceland, among others (Brown, 2015). If residents of these places wished to recycle their graywater, systems using porous volcanic rocks would be both easily accessible and relatively low cost.

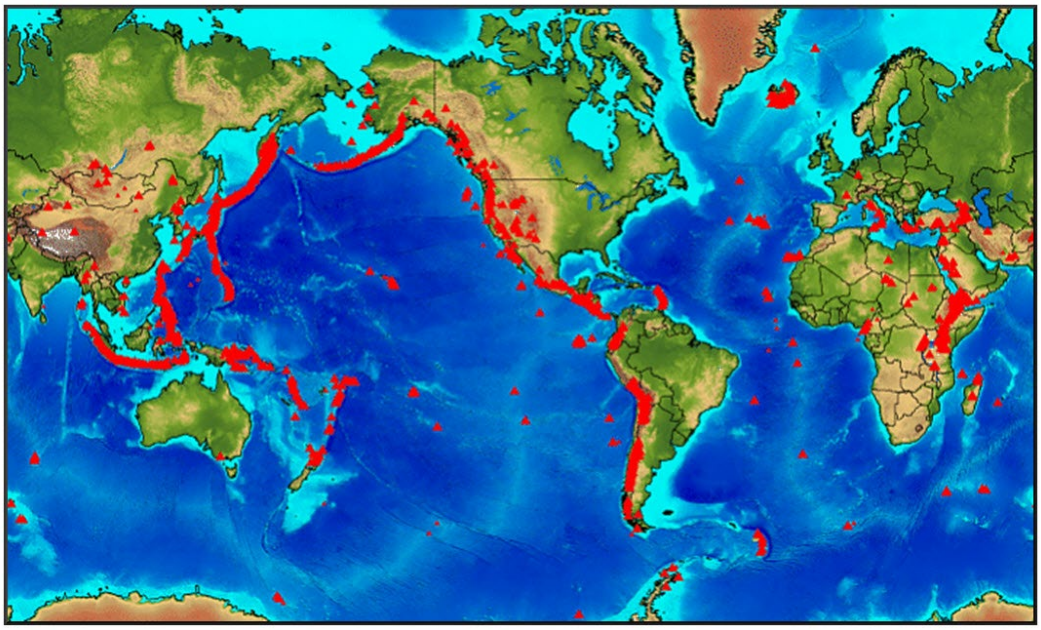

Figure 3: Map of major volcanoes worldwide, from CDC *Volcano Preparedness and Response program* (2022).

Red triangles symbolize major volcanoes. A majority of global volcanism occurs in the "Ring of Fire," circling the Pacific Ocean.

Project Introduction

Methods overview

The characterization of the pumice and scoria samples was conducted using a variety of instruments and techniques in Dr. Giachetti's Physical Volcanology lab. Using sieves, balances, a Particle Analyzer, and a helium pycnometer, I divided large batches of unsorted samples into well-defined size ranges and measured their mass, numbers of particles, volume, porosity, and density. Following these characterizations, I tested the basic interactions of the samples with water in static immersive settings, measuring the packing fraction of clasts and the absorption levels in both tap water and graywater. I created graywater following a simplified "recipe" in the lab; however, these experiments offer realistic predictions of what could be expected if these samples

were used as filtration media for real-world, domestically-generated graywater in an active flow setting. More specific information on these procedures will be described in the Methods section.

Sample information

The samples I used in my thesis project are pumices and scoriae that were collected in Central Oregon. Pumice samples were sourced from Mount Mazama, and scoria were sourced from a cinder cone near La Pine (see Figure 4). Mount Mazama, discovered by white settlers in 1852, is referred to in the native Klamath language as the former mountain of *Tum-se-ne*, in which rests *giiwas* (English name: Crater Lake) (Alatorre, 2021). Klamath oral tradition tells that *giiwas* was created after a fight between two spirits collapsed the top of *Moy-Yaina* (Mount Mazama), leaving behind the mountain *Tum-se-ne* and its caldera lake. Prior to the nineteenth-century influx of white settlers and the forceful displacement of native groups, what is now the La Pine area was inhabited for centuries by the Molalla people (*Whose Land*, 2021). The region has a deep human history; settlements dating back thousands of years have been uncovered on the nearby Newberry volcano (Oregon History Project.)

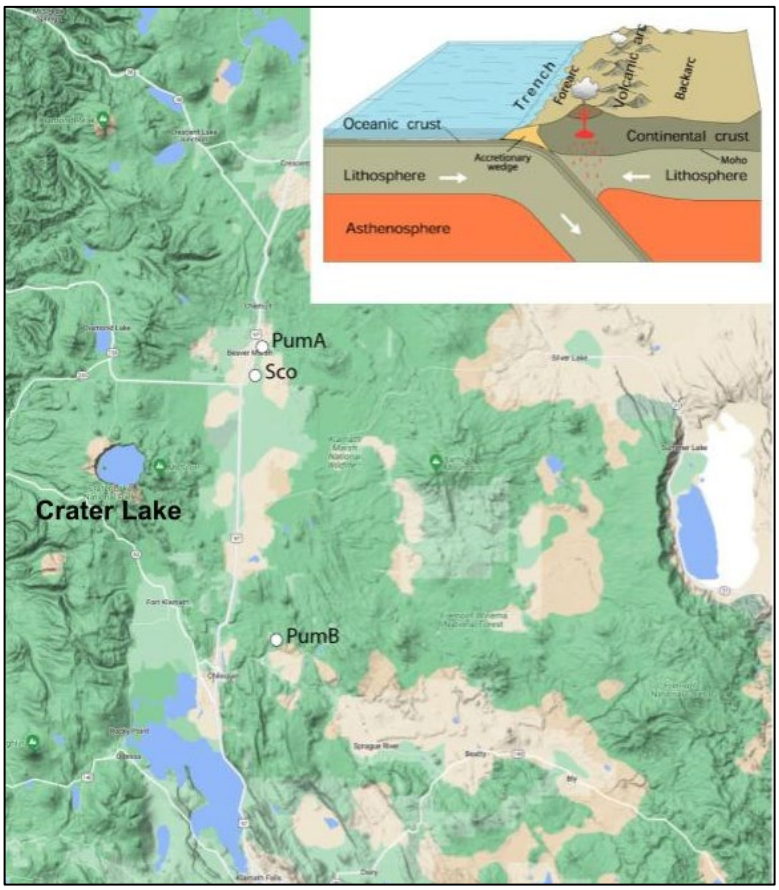

Figure 4: Map showing sample locations in relation to Crater Lake (Mount Mazama).

On left side of figure is Crater Lake. Locations of sample collection for each type are labeled. Inset shows tectonic diagram of subduction zone and creation of arc volcanism. See Figure 5 for regional map of Cascades volcanoes.

For the remainder of this thesis, the pumices are labeled and referred to as *PumA* and *PumB*, and the scoria are labeled and referred to as *Sco*. Both the scoria and the pumice samples were collected in the field and placed into large gallon-sized plastic bags, then brought back to the lab, after which my work began. Each sample set consisted of 4.2-9.3 kg of loose tephra ranging in size from <1 mm to a few centimeters.

Regional volcanic context

Both Mount Mazama and the cinder cones near La Pine are products of the same regional volcanic setting. Off the coast of Washington, Oregon, and northern California, a subduction zone occurs where two tectonic plates meet. The oceanic Juan de Fuca plate, to the west, is slowly sliding underneath the continental North American plate to the east in a process called subduction (see inset in Figure 4). As the oceanic plate moves deeper underneath the continent, the minerals within its rocks release water, triggering the melting of crustal rocks into lava. This lava, more buoyant than the surrounding solid rocks, rises through the Earth's crust to the surface, where it creates volcanoes in an "arc" parallel to the subduction zone but several kilometers inland from the plate boundary. The Pacific Northwest's famous Cascade Range is such an arc, a 1,100-km linear stretch of volcanoes from Lassen Peak in California to Mount Baker in Washington, as well as further north to the Silverthrone Caldera in British Columbia, Canada.

On a geologic scale, volcanoes in the Cascades are frequently active, with eruptions occurring every few hundred years on average (see Figure 5 for diagram of Cascades volcanoes and eruptions in the last 4000 years). Mount Mazama, the volcano which produced the pumices used in my project, underwent a major explosive eruption 7,700 years ago, forming a caldera which today is filled by Crater Lake; minor eruptive activity has occurred at the volcano since then but none as extreme as the caldera-forming eruption. In 2022, a new report was released by the USGS stating increased uplift at South Sister, near Bend, Oregon– suggesting the movement of magma around 7 kilometers below the surface (Lisowski, 2022). Although no hazardous volcanic activity

is thought to be imminent, the changes at South Sister are a reminder that the Cascades are an active volcanic region, and that the process which created the pumices and scoriae in my project still continue today.

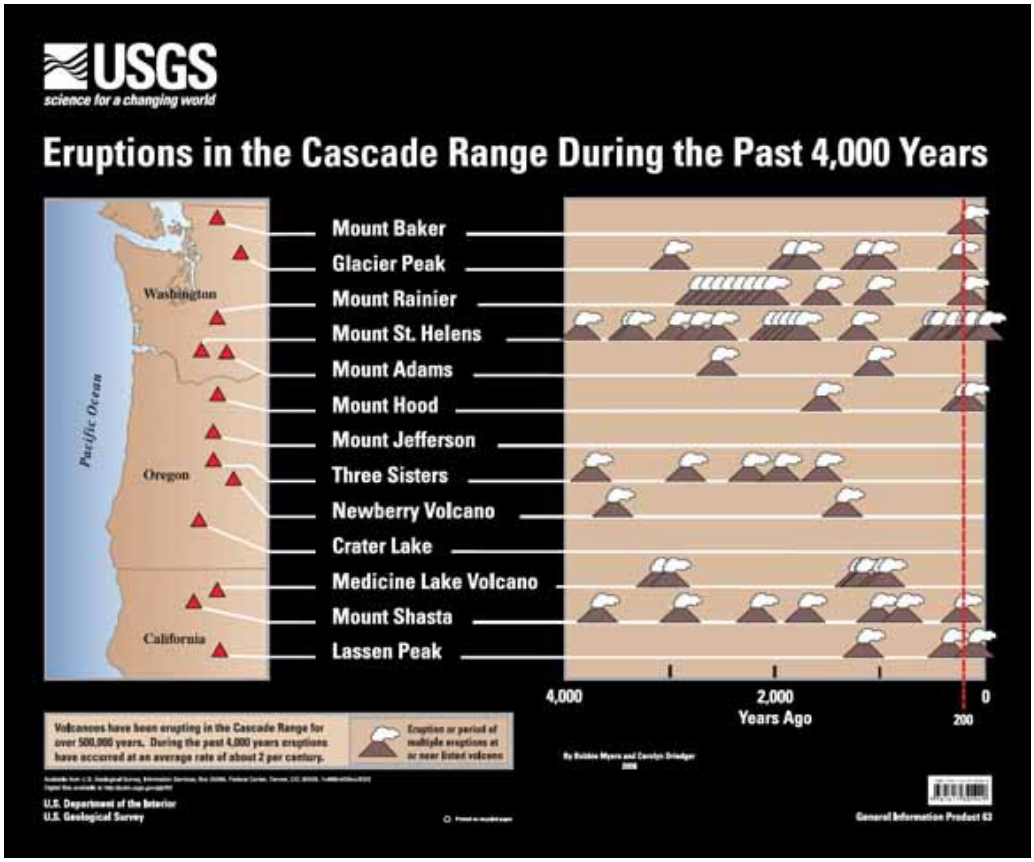

Figure 5: Map of major Cascades volcanoes, including Crater Lake (Mt. Mazama), and their eruptive histories over the last 4000 years. From Myers (2008).

Note that Mount Mazama has no recorded eruptive activity in the last 4000 years; its last major activity was 7,700 years ago, when a major, or "climactic," eruption destroyed its cone and resulted in the formation of the caldera and today's Crater Lake.

Methods

Methodological Overview

This project operated in two main phases. First, rock and water samples were collected and characterized in order to quantify as many details pertaining to filtration as possible. Second, rock samples were tested for their ability to absorb water in a passive-immersion setting. The reader is encouraged to review the experimental and analytical procedures detailed in Figure 6.

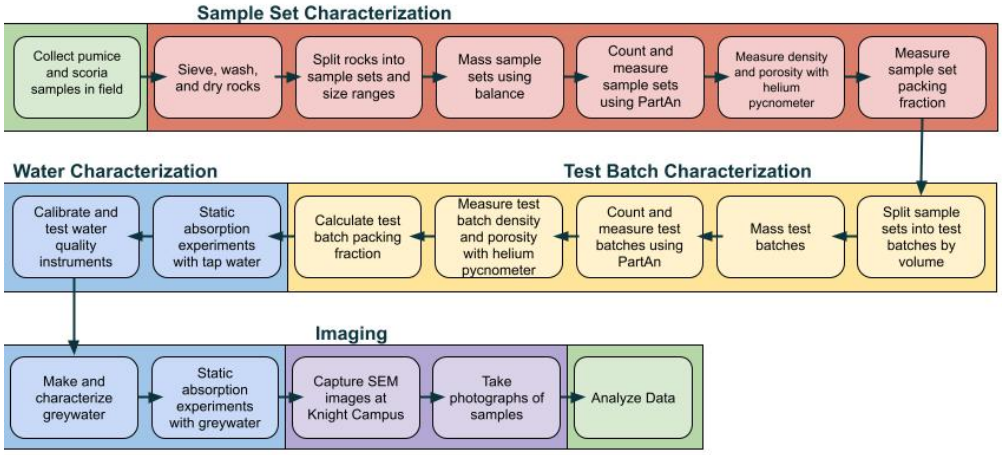

Figure 6: Methods flow chart

The methods used in this project are broadly categorized into four stages: sample set characterization, test batch characterization, water characterization, and imaging.

Rock Sample Collection

My project utilizes two pumice samples from Mount Mazama: one from the ~7,700-year-old caldera-forming (“climactic”) eruption and one from the Cleetwood eruption, which occurred a short time (i.e., days to decades) before the climactic eruption. The samples were collected by Dr. Giachetti and his graduate student Joshua

Wiejaczka, in the spring of 2021 and brought back in plastic gallon Ziploc bags. *PumA* samples were collected from the South Chemult Quarry in Chemult, Oregon, near Crater Lake National Park, while *PumB* samples (pumice from the earlier Mount Mazama Cleetwood eruption) were collected from a site around 45km SE of the vent which is thought to have been the source for the Cleetwood eruption.

The scoria were collected from a cinder cone around 3 km south of the South Chemult Quarry. Less is known about their age or origin because cinder cones are much smaller than stratovolcanoes and are more numerous, especially in the Cascades region. See Figure 4 for detailed locations of sample collection relative to Mount Mazama.

Much contemporary volcanology research has been done regarding the contamination of surface water sources with heavy metals leaching from volcanic eruptive materials. Such leaching is not thought to be a concern in the samples used in my thesis; existing literature shows that nearly all heavy metal leaching occurs shortly after eruption (Bosshard-Stadlin, 2017). The pumices and scoriae utilized in my project were erupted thousands of years ago and have since been subject to weathering through precipitation, thus currently posing no known threat of leaching heavy metals into effluent.

Primary Rock Sample Characterization Methods

Sieving

Before sieving, organic material, namely fragments of plant roots, was removed from the samples using tweezers. Each sample (i.e., *PumA*, *PumB*, and *Sco*) was then sorted into size categories using 8-inch round metal sieves. The sieves used had

spacings of 32 mm, 16 mm, 8 mm, 4 mm, 2 mm, and 1 mm. Sieves were stacked vertically from narrowest (bottom) to coarsest (top), and then a few handfuls of dry samples were poured from a bag into the top sieve (coarser). The sieves were then shaken manually for around five minutes so that smaller particles fell through coarser sieves until they found a resting place between two sieve sizes. Once thus sieved into size categories, the clasts were placed in bags with others of their size range. This process resulted in five particle size fractions used for experiments: 16-32 mm, 8-16 mm, 4-8 mm, 2-4 mm, and 1-2 mm. Particles smaller than 1 mm were not used in the experiments. *PumA* did not contain enough particles 1-2 mm to be used in the experiments.

Washing and drying

Sieving or any other form of physical manipulation creates dust through abrasion– during movement (including shaking of the sieves), clasts rub against one another, grinding small pieces of dust. This is particularly true of pumices, because glassy bubble walls are thinner than in the scoria. Once sorted into size categories, samples were thus washed to remove dust. Washing was done using beakers and sieves: first, clasts were shaken lightly in a sieve to dislodge dust; secondly, tap water was run through the sieve; lastly, the wet clasts were removed from the sieve and placed in a beaker. The beaker was filled with water, stirred, and drained so that further dust was removed with the water. This process was repeated multiple times, until it seemed that most of the dust had been removed from the samples. Due to constant abrasion while manipulating dry and wet particles, it was never possible to remove 100% of the dust.

After draining the beaker used in washing, the wet clasts were placed in an oven, where they dried for around 24 hours at 120 C. After drying, samples were set aside to cool down to room temperature and then were placed in new plastic bags sorted by size category.

Removal of Outliers

Each sample set contained a small number of clasts which, although deposited and harvested with the pumice or scoria, were different kinds of rocks, such as obsidian in the pumice samples or pumice in the scoria samples (i.e., lithics). These outliers were manually removed following the drying stage, typically with tweezers. This sorting was conducted for all samples larger than 2mm in size.

Mass

Mass was measured for each size fraction using a balance with a precision of 0.1 g and a maximum mass of 500 g.

Sample Photography

Examples of particles for each size fraction and sample were photographed against white paper using a digital camera and a scale bar (Figure 7).

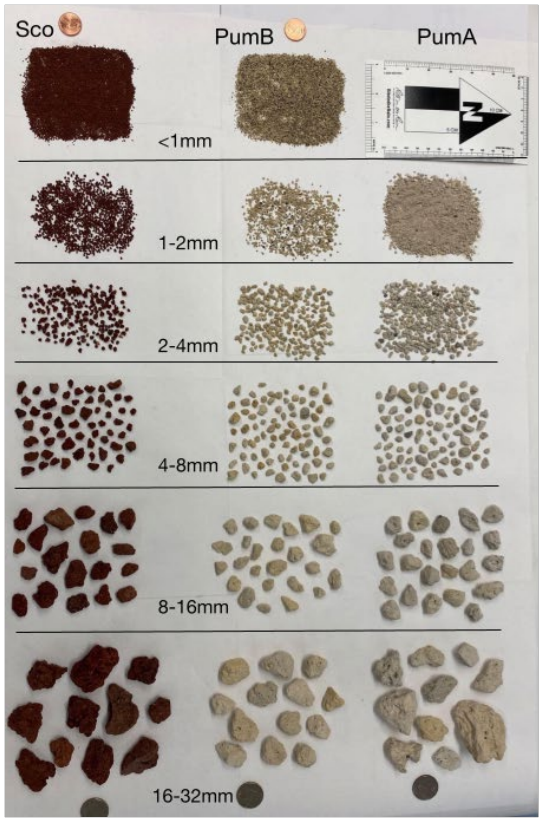

Figure 7: Comparison of Sco, PumB, and PumA samples. Pennies, quarters, and a geologic scale bar are included for scale.

Samples of *PumA* and *Sco* were made into thin sections by Spectrum Petrography Inc. and imaged using the Scanning Electron Microscope in the University of Oregon Knight Campus– see Figure 8– to obtain a deeper understanding of the microscopic physical appearance of the pores in addition to the macroscopic physical appearances of the clasts.

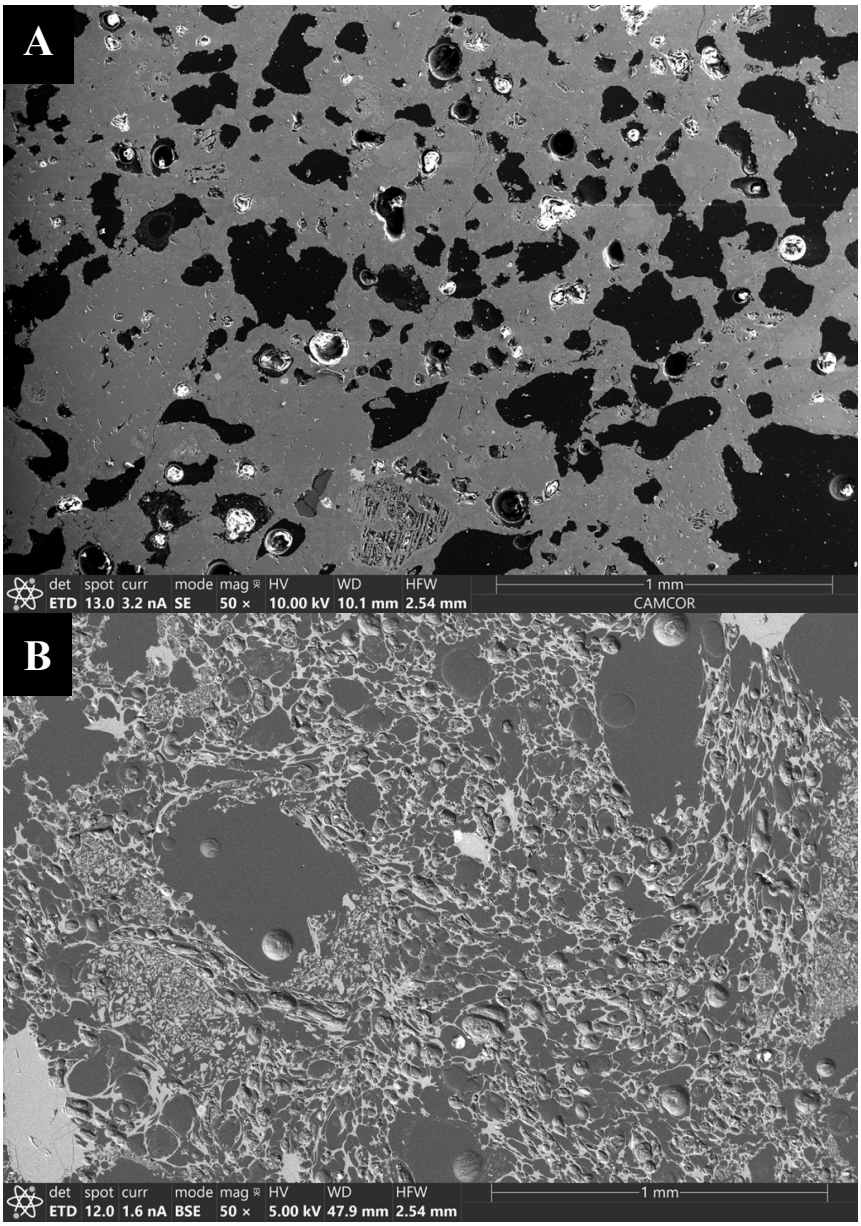

Figure 8: Scanning Electron Microscope (SEM) images of 8-16 mm Sco (A) and 8-16 mm PumA (B), both taken at 50x magnification. Photographed with the assistance of Kurt Langworthy in the Knight Campus SEM. In both images, the lighter gray material is solid-phase rock, while the darker material is void, or pore space. 8-16 mm Sco have total porosity of 65.2% and 8-16 mm PumA have total porosity of 86.3%; this difference can be clearly seen when comparing these two images. Both images were taken with magnification of 50x. The bubbles in the Sco sample are notably larger and less tortuous than those observed in the PumA sample.

Secondary Rock Sample Characterization Methods

Particle Size Analyzer

All size fractions of the three samples were analyzed using a MicroTrac Particle Analyzer (PartAn^{3D}) instrument. The PartAn^{3D} is based on Dynamic Image Analysis. The instrument is operated by placing particles on an elevated vibrating metal tray, which directs the particles to fall across the view of a high-resolution, high-speed camera (Figure 8). The camera captures several 2D projections of each particle and then uses an algorithm to calculate the 3-dimensional length, width, thickness, surface area, volume, sphericity, and circularity (and many other shape parameters) of each particle. For samples <4 mm, a 20-mm-width vibrating tray was used, whereas a 60-mm tray was used with larger particles. Each size fraction was put through the PartAn at least three times, to obtain averages and account for minor errors in counting (caused, for example, by one clast falling in front of another such that the camera either does not detect the clast in the back or counts the two as just one larger particle). Using these data, we can calculate the total volume of particles within a size fraction by adding the individual volumes of all particles. Data from the PartAn was saved in Excel files (with one line of size and shape parameter per particle) and synthesized into separate documents. Additional information about the MicroTrac Particle Analyzer instrument can be found in Trafton (2021) and Wiejaczka (2022).

Data from the PartAn was further analyzed to consider trends in physical characteristics between size fractions. For each size fraction run through the instrument, values for important parameters were compiled and then analyzed to find medians, averages, and standard deviation. These values were plotted in order to look for

connections between sample types and size fractions. The parameters most important in these analyses are solidity and convexity. Solidity measures the degree to which the surface of a particle is smooth; a perfectly round particle with no texture or vertical variations would have a solidity of 1.0, or 100%. Convexity is a measurement of the degree of outward curvature of a particle; a particle with a convexity of 1.0 or 100% would be perfectly spherical.

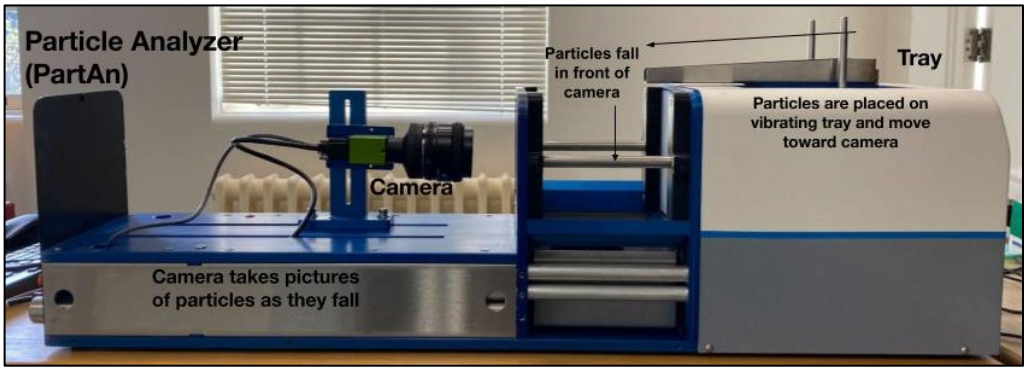

Figure 9: Labeled photograph showing MicroTrac Particle Analyzer function.

In using the PartAn, pumice and scoria clasts were placed on the vibrating tray and fell in front of the camera, which recorded data about their physical characteristics based on 2-D photographs.

Helium Pycnometer

Density and porosity measurements were obtained using helium pycnometry in Dr. Giachetti's lab. In this procedure, samples are placed in a chamber calibrated for its volume. The chamber is then first evacuated of air and filled with helium, which has small enough atoms to be able to fill all interconnected pores, whether they are bubbles in the particles that are connected to each other and to the exterior of the particle, or pore spaces in between individual grains. The instrument provides the volume inaccessible to helium (i.e., solid volume and isolated pores). Measuring finely crushed

samples (i.e., broken glass that does not contain any bubbles) using helium pycnometry allows for the quantification of the volume of solid, which can then be used together with the mass of the powder to calculate the density of the solid phase. Using the density of the solid phase, the mass of the raw particles, and their total volume measured using the PartAn3D, we can calculate the total (bulk) porosity of the size fraction. Analyzing the raw particles using helium pycnometry allows for a quantification of the volume of solid and isolated (closed) pores, which is used to calculate the connected (open) porosity. A detailed explanation of the calculations used to find porosity and density with helium pycnometry data can be found in Appendix 1.

Packing Fraction

Packing fraction is a measure of how closely particles in a space are stacked together. The packing fraction of a system is the proportion of space which is occupied by the particles in question (as opposed to void in between particles). Packing fraction data was collected for each sample type and size fraction by filling a beaker with a measured volume of clasts (e.g., 500 cm^3), then running those same clasts through the PartAn to obtain their collective volume (e.g., 410 cm^3). The packing fraction is obtained by dividing the total volume of particles by the volume of the container (e.g., 410/500=0.82).

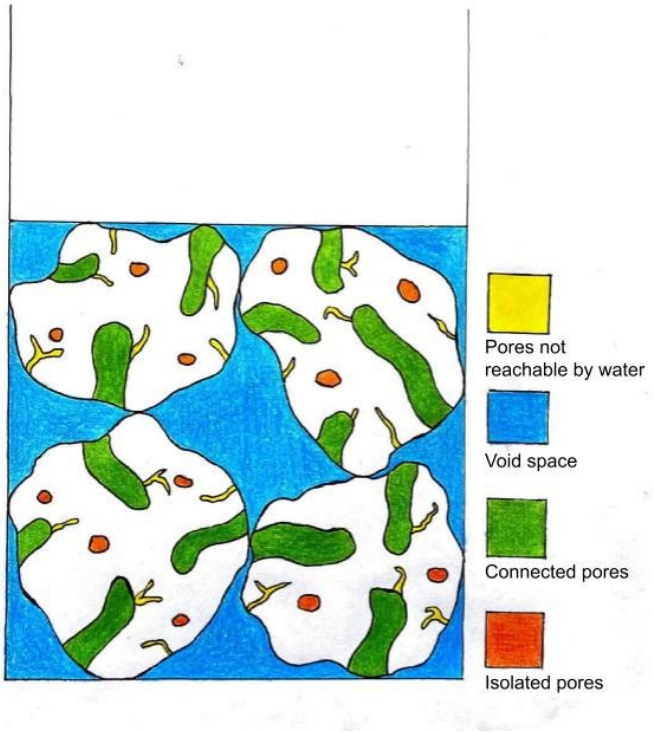

Figure 10: Diagram showing different types of spaces in a container with idealized porous rocks and water.

Packing fraction is calculated by diving the volume of space occupied by rocks by the total volume (rock space plus blue space). Blue represents void space around the rocks which is filled with water. The red bubbles represent isolated pores, filled with gas and surrounded by solid material– technically pore space but unable to be accessed by water. Green spaces represent connected pore space which is open to the outside and can be reached by water. Yellow spaces represent pores which, as measured by the helium pycnometer, are connected to the exterior but are too convoluted or small to be penetrated by water molecules.

Water Sample Characterization

To conduct experiments with tap water and graywater, it was necessary to quantify characteristics of the water before the experiments in order to measure changes. Several water quality parameters were quantified using multiple instruments

and test methods. After introductory testing and calibration, characteristics of both tap water and graywater were measured using these instruments.

Water quality parameters

The water quality parameters tested in this project were pH, turbidity, nutrient content, total dissolved solids (TDS), conductivity, and temperature. Units, measurement techniques, calibration information, and typical values for each parameter are explained in detail below.

- **Turbidity**: Turbidity is a measurement of the clarity, or amount of suspended particles, within a liquid. This parameter is typically measured in NTU (nephelometric turbidity units), with high turbidity values relating to high amounts of suspended particles. Drinking water, ideally, has a NTU of 0. The SGZ-200BS Portable Turbidity Meter used in this project required a collection of a ~50 mL sample of water, and was calibrated using a 200 NTU standard. The instrument can measure values between 0 and 200 NTU.

  Turbidity readings were taken by agitating a small vial of sample water and then inserting it into the instrument to be optically analyzed. Typically, readings begin high and then drop until they stabilize within a few minutes; this is due to the settling of large particles. The manual for the unit suggested to take measurements after 10 seconds. In these experiments, turbidity was recorded both at the 10-second mark and once the reading settled.

- **Conductivity**: Conductivity measures the ability of water to carry an electrical current. The BlueLab conductivity pen used in this project measured conductivity using EC (electrical conductivity) units. Conductivity is also frequently measured in units of Siemens/meter or microSiemens/centimeter. Typical values for drinking water conductivity are around 200-800 microS/cm. The conductivity pen was calibrated using a 2.77 EC standard solution.

- **Nutrient Content**: The BlueLab nutrient meter used in this project measures the amount of dissolved nutrients in water with units of parts per million, a typical unit. This instrument calculates nutrient levels from conductivity readings, and its manual and seller website do not specify which nutrients are being studied. Typical clean drinking water has low nutrient content, and the highest permissible nutrient level is around 400 ppm. The manual was not specific as to which nutrients (i.e., phosphorus, nitrogen, etc.) were being measured.

- **Temperature**: Temperature is recorded in Celsius using the Multifunction meter. Water at room temperature typically is around 20 degrees C.

- **TDS (total dissolved solids):** TDS is a parameter characterizing the amount of particles that are dissolved in solution. The Multifunction meter used in my project records TDS in parts per million. This project's TDS meter was calibrated using a 12.88 mS/cm solution. Typical recommended TDS values for drinking water are below 300 ppm, or 468 mS/cm.

- **pH**: pH measures how basic or acidic a substance is and is measured on a scale from 0 (being most acidic) to 14.0 (most basic), with 7.0 considered neutral. The Multifunction pH meter was calibrated using three solution standards of pH 4.0, 6.86, and 9.81. Typically, pure water has a pH of 7.0, but some range is observed in drinking water due to variations in chemical and mineral content.

Graywater components, creation, and characterization

The graywater was prepared in the lab using conventional cleaning and personal care products purchased from a grocery store. Amounts of each product were determined from a simplified graywater "recipe" provided by a researcher with local company Leapfrog Design; the recipe is derived from the NSF (National Sanitation Foundation) 350 Challenge graywater mixture (see recipe in Table 1). This particular graywater mixture does not contain food particles or hair, two typical components of graywater, to eliminate potential clogging issues associated with large particles. The recipe also was originally portioned to make 100 L but was scaled down to a 10 L batch for the experiments in this project. Each component was measured using a high-precision scale (0.0001 g precision) and then added to the 5-gallon bucket, in which 10L

of tap water was placed. The components were incorporated into the water using a hand mixer with a whisk attachment at high power for several minutes. After being mixed, the bucket was sealed and stored at room temperature for around two months in the laboratory until experiments began.

Table 1. Graywater recipe and ingredient proportions

Ingredient	**Mass (g) / 10L**
Body wash w/ moisturizer	3
Liquid hand soap	2.3
Conditioner	2.1
Shampoo	1.9
Bath cleaner	1
A2 fine test dust*	1
lactic acid	0.3
toothpaste	0.3
deodorant	0.2
total mass (g)	12.1

* The A2 fine test dust meets ISO 12103-1 standards. Obtained through personal communication from Markus Koeneke.

Volume-equivalent samples of graywater, tap water, and distilled water were tested for the above water quality parameters to establish baseline patterns between the three types of water.

Implementation of water quality measures

Prior to beginning the absorption experiments, graywater, tap water and distilled water were characterized to establish baseline values and understand the main experimental and compositional differences between the types of water. The generic-brand distilled water used was purchased at a store; the tap water was obtained from the

faucet in the laboratory. Tap water in the Eugene-Springfield area is sourced from the McKenzie River and treated by the Eugene Water and Electric Board (EWEB).

Static Absorption Experiments

Following characterization of the rock and water samples, a series of experiments was conducted to investigate the interactions between samples and water in static immersion settings (settings in which there was no flow or constant fluid motion).

Isolation of Experimental Test Batches

To account for variations in volume between sample sets and to ensure methodological consistency, all sample sets were divided into smaller "test batches", which were used for all following experiments. Test batches were determined based on collective volume when measured in a graduated cylinder. Each size fraction from every sample set was split into a test batch except for the 16-32mm *PumB* size range (there were only 49 clasts in this size fraction– not enough material for a separate test batch). Thus, there were four *PumA* test batches (ranging from 2-4 mm to 16-32 mm), four *PumB* test batches (1-2 mm to 8-16 mm), and five *Sco* test batches (1-2 mm to 16-32 mm).

Table 2: Test batches, amounts of water added, and container volumes. Volumes of test batches and water added were scaled with the increasing size fraction particle size.

Size fraction of rock	Volume of test batch	Volume of water added	Size of graduated cylinder
1-2 mm	100 mL	90 mL	250 mL
2-4 mm	200 mL	175 mL	500 mL
4-8 mm	400 mL	350 mL	1000 mL
8-16 mm	800 mL	700 mL	2000 mL
16-32 mm	1600 mL	1400 mL	2000 mL

Mass, external volume, porosity, density, and packing fraction were re-measured for each test batch using the same methods described for the collective sample sets. Data from these measurements showed consistency between test batches and their source sample set size range, suggesting that the test batches were representative of the entire size fraction. After these measurements, test batches were used in static absorption experiments with both tap water and graywater. Test batches were doubled in volume for each increase in clast size range; the amount of water added in the experiments was also doubled with each size progression. See Table 2.

Static Tap Water Absorption

Tests were conducted to quantify the tap water absorbed by pumices and scoriae in a static setting. The absorption of water by clasts can inform about potential sample-water interactions in an active-flow setting. These tests were performed in two stages.

In the first stage, glass beakers were filled to a marked volume with clasts of known total mass, then tap water was added until the water level reached a further marked volume. The beaker was then covered and placed in a cool location to prevent evaporation, and its total volume was monitored and measured at 1-minute, 2 min., 5 min., 10 min., 30 min., 60 min., 2-hour, 6-hour, and 24-hour marks to observe decreases in water volume due to absorption by the rock samples. After volume was measured at the 24-hour interval, the water was removed, and the saturated clasts were massed again to calculate the mass of water absorbed within the rocks' structures. Measuring this absorption informs conclusions about how similar rocks would potentially absorb water in an active flow system, and thus how much water would be in contact with the rocks' interior and exterior surfaces to be filtered.

In the second stage, plastic graduated cylinders were filled to a marked volume with the test batches of each size fraction. Then, a controlled volume of water was added to the cylinder, and the total volume measured immediately, so that the amount of water absorbed by the samples immediately upon immersion could be recorded. Water volume in the cylinder was measured at the same time intervals as in the previous stage. After 24 hours had elapsed, the remaining water was poured out into another graduated cylinder and measured, thus allowing observation of the change in volume between the water added initially and water remaining. Like in the first stage, the clasts were weighed after being immersed to measure their change in mass, presumably caused by absorption of water. After these steps, the clasts were dried in the oven, and then weighed again once dry to see any change in mass from initial measurements.

Pumice Restrained Immersion System

During the initial stage of static immersion experiments, it was observed that, due to their density, most large pumice clasts floated. This became especially problematic in the second stage of experiments, conducted in graduated cylinders. For pumices larger than 4 mm, several clasts would be uplifted by other floating clasts so that they were not immersed in the water at all. Since this experiment's design assumes that all clasts are fully submerged, it was essential to force all clasts to be completely underwater for the duration of the trial. This was accomplished through the design of a restrained immersion tool.

A circle of fine mesh (finer than the pumice size but coarse enough for water to freely pass through) the diameter of the graduated cylinder was attached to the end of a wooden dowel. The dowel was cut to a length so that the height of the sample column

would be below the minimum water level. A bar was adhered to the other end of the dowel, so that the tool could be secured with tape such that it would not rise upward due to the buoyancy of the pumices. A tool using this design was constructed for each of the five size ranges which required it (*PumA* 4-8 mm, 8-16 mm, and 16-32 mm; *PumB* 4-8 mm and 8-16 mm). This design allowed all clasts of pumice to be totally immersed in water for the entire duration of the experiment. See Figure 11.

Figure 11: Restrained immersion tool.

The tools used for keeping pumices from floating were composed of wooden dowels and fine mesh circles attached together.

Because the restrained-immersion tool was composed largely of wood, it was expected to absorb a small amount of water when immersed. Each tool was thus weighed before and after immersion to track any changes in mass resulting from water absorption. These changes were considered in data analysis following the conclusion of the experiments.

Tap Water Absorption Calculations

Following the conclusion of the absorption experiments, a series of calculations was conducted to measure several water-rock interaction parameters. Using data from

the static absorption procedure (mass of dry samples, the volume of water added, changes in water volume within the graduated cylinder, and the sample packing fraction), I calculated the following: the volume and relative proportion of "available" void space in the system which water could theoretically reach (i.e., void space in between particles and within the particles themselves); the total mass and relative proportion of water absorbed into the rocks before and after the water was poured out; the volume of water absorbed; the fraction of container volume occupied by water (both in and around clasts); the ratio of water absorbed to water added; the ratio of change in water level after 1 minute to the amount of water added initially; and the proportion of clasts' connected pores which actually were permeated by water. See Appendix 2 for a detailed explanation of these calculations.

Supplementary Tap Water Absorption Experiments

In addition to the 24-hour static absorption experiments, which were conducted for every test batch, two smaller experiments were conducted to investigate water activity over longer time scales. To investigate whether meaningful absorption happens beyond 24 hours, a 1000 mL beaker was filled with 500 mL of 8-16-mm *PumA* clasts and with 1000 mL of tap water, covered, and left in a cool, dark place for three weeks.

Another additional experiment was carried out in which 1000 mL of tap water was put into a graduated cylinder, covered, and left in a dark place for five days. This experiment was designed to show if any meaningful evaporation of water occurred on the scale of days in the typical climatic settings of the lab, so that any water loss through evaporation could be accounted for.

Static Graywater Absorption

Experiments testing static immersion interactions with graywater were conducted in a method mirroring those which were conducted with tap water. However, in addition to monitoring all the same data as the tap water experiments, the graywater experiments also included water quality measurements of the graywater before, during, and after immersion with the rock samples.

Prior to the experiment, each test batch was sieved (to reduce dust) and then massed. Test batches were gently placed in graduated cylinders with a paper towel coating the inside of the container (also so as reduce dust). If the samples required a restrained immersion device, it was inserted and attached to the graduated cylinder using duct tape. Graywater was rigorously stirred to ensure homogeneity, then tested for the water quality parameters listed above (pH, temperature, TDS, conductivity, nutrient content, and turbidity). A measured volume of this graywater was then poured into the cylinder over the top of the rock column. A separate cylinder of an identical amount of graywater was placed alongside the rock-and-graywater cylinders to provide a control sample.

After 1 hour, the level of water in the cylinder was recorded, then the graywater was poured out (using a mesh screen to keep the rocks in the cylinder) into a separate container and measured for volume and the above water quality parameters. The control sample of the graywater was stirred and then sampled in the same way. Following these measurements, the graywater was poured back into the cylinder over the rocks. This procedure was repeated at the 3-hour mark, then after 1, 3, 5, and 7 days. After taking final graywater quality measurements on the seventh day, the graywater samples were

removed from the graduated cylinders and placed in closed containers for potential future sampling. The graywater-saturated rocks were massed, dried, and massed again.

Due to limited supply of graduated cylinders, the static graywater absorption experiment was not conducted for the 16-32 mm size fraction of *PumA* samples.

Results

Collective Sample Set Mass

Material less than 2 mm in diameter constitutes only 3.52% of the total *PumA* sample set mass and is principally composed of fine dust. This material is not characterized nor used in experiments. In contrast, nearly half the mass of *PumB* is clasts less than 2 mm diameter, with much of this mass being intact clasts. For this reason, these smaller particles were further sieved to create a 1-2 mm size range for use in experiments. There is also enough sizeable material of the *Sco* sample set between 1-2 mm to justify creating a fifth size range. See **Table 3** for mass measurements.

Table 3: Mass, volume, and clast count data for the entire *PumA*, *PumB*, and *Sco* samples.

		Mass (g)	Volume (mm^3)	Number of clasts	Avg. clast mass (g)	Avg. clast volume (mm^3)
PumA	2-4 mm	662.1	1,598,780.7	65245	0.010	24.5
	4-8 mm	1314.47	3,452,556.8	24750	0.053	141.6
	8-16 mm	1743.52	5,257,093.8	4938	0.353	1067.6
	16-32 mm	545.44	1,871,522.3	285	1.913	6536.0
	total	3720.09	12,179,953.6	95218		
PumB	1-2 mm	1107.3	1,797,916.9	1107	0.002	2.5
	2-4 mm	1681.3	3,671,723.0	1681	0.005	13.0
	4-8 mm	1065.2	2,271,426.5	1065	0.053	113.8
	8-16 mm	401.5	994,821.1	401	0.364	781.9
	16-32 mm	49.7	164,777.2	49	1.380	4577.1
	total	4305	8,900,664.7	4303		
Sco	1-2 mm	651.5	559,167.9	651	0.003	2.5
	2-4 mm	1504.47	1,483,046.5	1504	0.016	16.2
	4-8 mm	1803.88	1,815,659.4	1803	0.152	153.8
	8-16 mm	2234.4	2,234,570.5	2234	1.255	1255.6
	16-32 mm	1960.98	1,972,274.5	1960	7.209	7256.2
	total	6194.25	8,064,718.8	8152		

Collective Sample Set Volume

In total, *PumA* is $1.2x10^7$ mm^3, the distribution of which follows the *PumA* mass distribution pattern. *PumB* is much less voluminous, $8.1x10^6$ mm^3. The *Sco* sample set has a total volume of $8.9x10^6$ mm^3.

Number of Clasts

The number of clasts presented in Table 3 for size fractions below 8 mm is an average of the number of clasts measured throughout all three runs in the PartAn. For size fractions 8-16 mm and 16-32 mm, particles were counted by hand.

In each size fraction, there may be a number of clasts that have certain dimensions larger than the bounds of that size fraction (e.g., particles with a dimension >4 mm in the 2-4 mm size fraction). This is because, during sieving, a clast that is 5 mm long in one dimension but 3 mm long on the two others may fall through the 4 mm sieve and be counted in the 2-4 mm size category, even though it has dimensions beyond those limits.

Average Clast Mass and Volume

The material used in this project, across all three samples and all utilized ranges, contain a collective mass of 16.73 kg and a collective volume of $29x10^3$ cm^3. Average masses and volumes for clasts in each size range were calculated using the number of clasts and the measured collective mass or volume for each entire size category. See Table 3.

Additional PartAn Data

The compiled PartAn data show relevant variations in convexity and solidity between size fractions and by sample type. Both parameters are consistent between the two pumice samples, with the pumices having higher values than the scoriae. Solidity values increase notably with size in *Sco* samples but increase only slightly in *PumA* and not at all in *PumB*. Convexity values throughout all three samples decrease as size increases, with *PumB* having slightly higher values than *PumA*. See Figures 12 and 13.

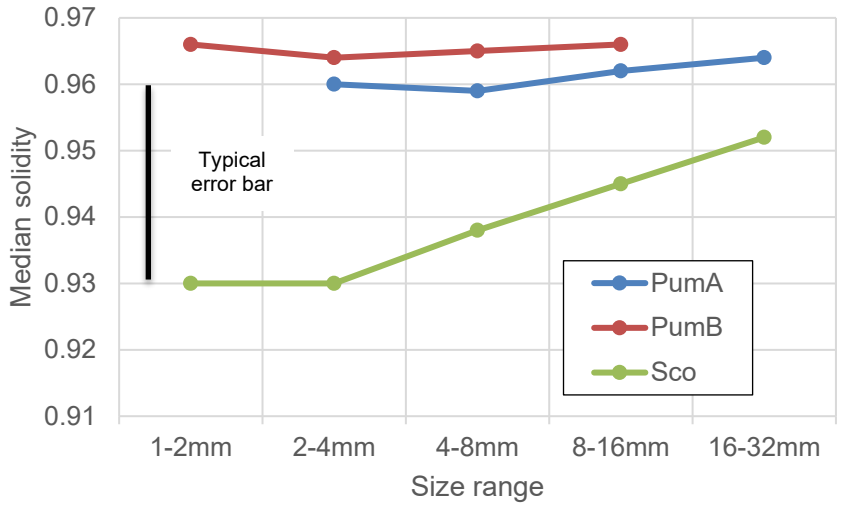

Figure 12. Median solidity by size range and sample type.

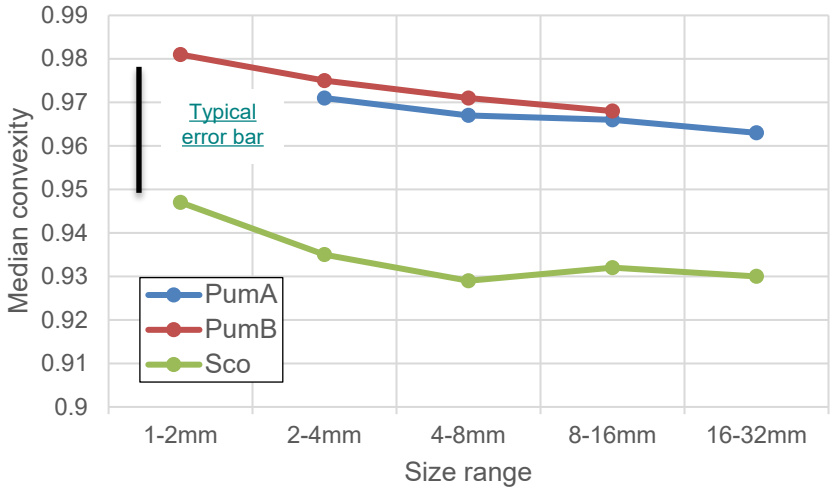

Figure 13. Median convexity by size range and sample type.

Density and Porosity

The solid phase density of the two pumice samples, as expected, is lower than that of the scoria: *PumA* and *PumB* densities range from 2.45-2.48 and 2.44-2.48 grams per cubic centimeter, respectively, while *Sco* density ranges from 2.85-2.86. For both pumices and the scoria, larger clasts are in general less dense than the smaller ones. Overall, scoria clasts show lower total, connected, and isolated porosity than pumice samples. Porosity varies minimally with size for both sample types but is highest in

pumices in larger sizes and in scoria within the 2-4 mm size fraction (Table 4). Figures 14 and 15 contain total and connected porosity variations between size fractions and sample types. See Figure 8 (SEM images of scoria and pumice) for a visual representation of different porosities.

Table 4: Results from test batch characterization by sample type

PumA	**2-4 mm**	**4-8 mm**	**8-16 mm**	**16-32 mm**
Mass (g)	68.5	118.5	211.7	338.5
Volume (mm^3)	156,824	314,195	627,014	1,035,095
Packing Fraction	0.784	0.785	0.783	0.646
Total porosity	0.824	0.848	0.863	0.867
Connected porosity	0.793	0.814	0.854	0.864
Solid state density (g/cm^3)	2.48	2.48	2.46	2.45
Usable void fraction	0.84	0.85	0.89	0.91
Volume fraction water	0.59	0.53	0.48	0.57
Effective porosity	0.66	0.8	0.52	0.72
Mass lost in TWA* (g)	-0.3	-2.1	-3.9	-4.1

PumB	**1-2 mm**	**2-4 mm**	**4-8 mm**	**8-16 mm**
Mass (g)	51.8	71.5	119.2	211.1
Volume (mm^3)	79,988	149,353	297,765	609,400
Packing Fraction	0.799	0.746	0.744	0.761
Total porosity	0.739	0.804	0.836	0.858
Connected porosity	0.703	0.773	0.806	0.832
Solid state density (g/cm^3)	2.48	2.44	2.44	2.44
Usable void fraction	0.76	0.83	0.86	0.87
Volume fraction water	0.69	0.66	0.56	0.52
Effective porosity	0.71	0.64	0.78	0.56
Mass lost in TWA* (g)	-0.5	-0.4	-2.9	-5.2

Sco	**1-2 mm**	**2-4 mm**	**4-8 mm**	**8-16 mm**	**16-32 mm**
Mass (g)	94.7	170.9	333.4	624.4	1192.9
Volume (mm^3)	84,545	160,486	339,661	629,051	1,171,363
Packing Fraction	0.845	0.802	0.849	0.786	0.732
Total porosity	0.608	0.628	0.656	0.652	0.643

Connected porosity	0.611	0.655	0.651	0.643	0.653
Solid state density (g/cm^3)	2.86	2.86	2.85	2.85	2.85
Usable void fraction	0.67	0.72	0.7	0.72	0.75
Volume fraction water	0.55	0.46	0.35	0.36	0.39
Effective porosity	0.86	0.78	0.86	0.81	0.77
Mass lost in TWA* (g)	-0.4	-0.4	-0.8	-1.9	-2.4

*TWA: Tap Water Absorption experiments.

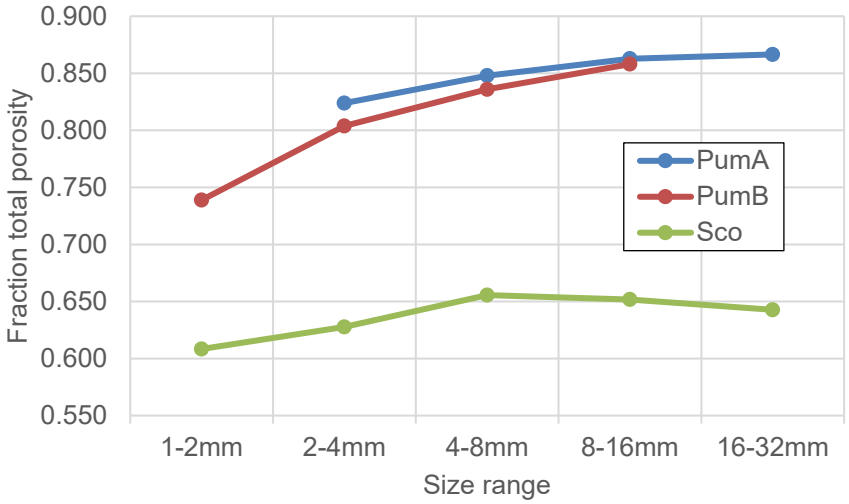

Figure 14: Total porosity

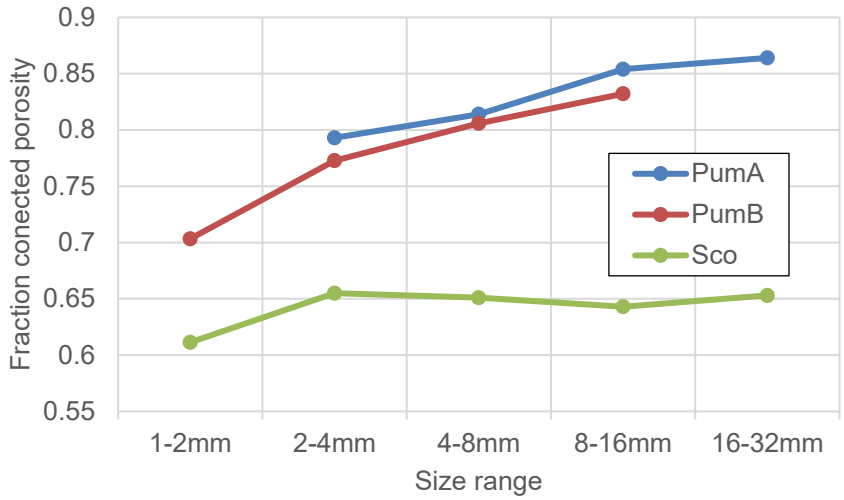

Figure 15: Connected porosity

Packing Fraction

Throughout all three sample sets, packing fraction (see Table 4) decreases with size. It is similar between pumice samples, and higher in scoria. Packing fraction was not recorded for the 16-32 mm size fraction of *PumB* because there was not enough material to complete the experiment. In pumice samples, packing fraction ranges from 0.64-0.78 (*PumA*) and 0.74-0.79 (*PumB*). Scoria packing fraction range from 0.83-0.91. See Figure 16 for a plot of packing fraction values.

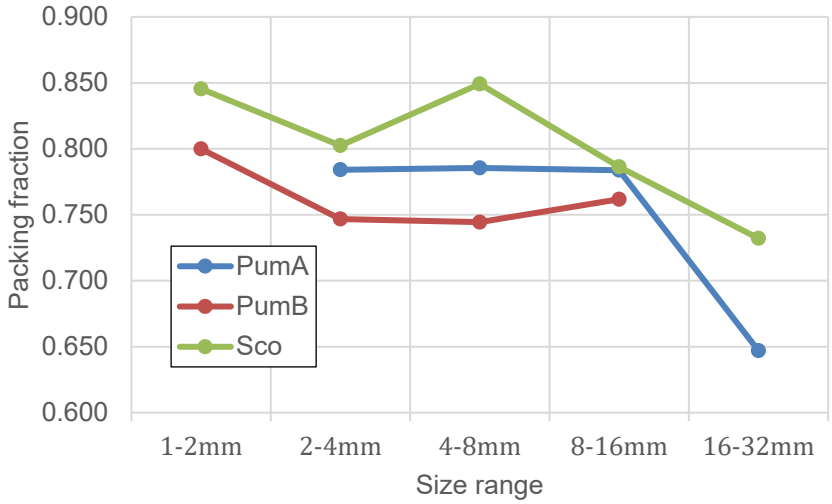

Figure 16: Packing fraction

Static Tap Water Absorption

The first static absorption experiment is not effective in determining the amount of water absorbed by the rocks for two reasons. First, the amount of water remaining in the system after 24 hours is not measured– only the change in mass between dry clasts before the experiment and water-saturated clasts afterward. We believe that, while pouring out the water at the end of the experiment (by tilting the graduated cylinder), water that has been absorbed into the rocks' pore space is being drained back out, thus leading to an underestimation of the amount of water effectively absorbed. Second, we observe floatation of pumices (especially the largest) in this preliminary experiment; this was remedied using the immersion device described earlier and in Figure 11.

In the revised static absorption experiments, the volume fraction of connected pores filled with water (Figure 17) is found to be higher in scoria (77-86%) than in pumices (56-80%). In other words, 20-44% of the pores in pumice (and only 14-23% in scoria) that are connected to the exterior of the particles are not filled with water, probably due to the narrow size of these pores/bubbles. However, the total amount of

water that can be added to a container full of pumice or scoria (i.e., both water entering the connected pores of the particles and water resting in between particles) (Figure 18) is higher for pumice (48-69%) than for scoria (35-55%). For both types of samples, smaller size fractions show a higher proportion of water filling connected pores and exterior void space than coarser particles.

In all samples, the total change in water volume before and after being poured into the rocks is significantly more than the observed decrease in water volume throughout the 24-hour period. This suggests that most of the absorption of water into clast structure occurs immediately upon immersion– the moment in which the water is being poured over the clasts.

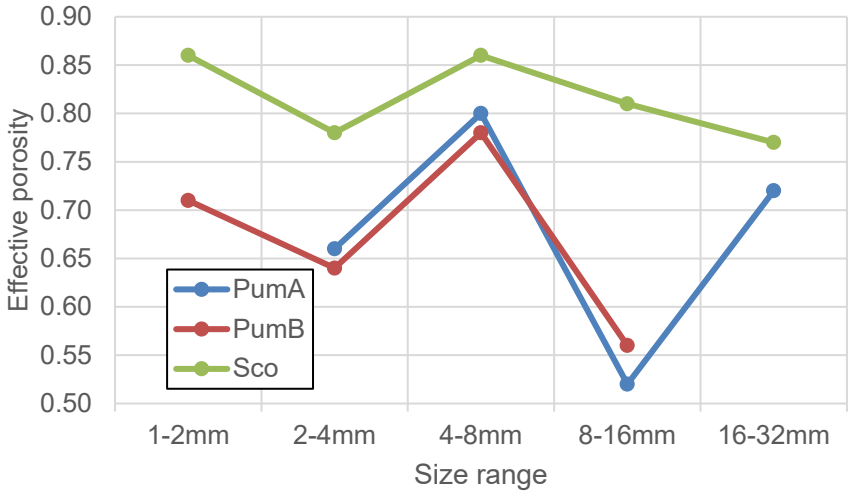

Figure 17: Fraction of connected pores filled with water

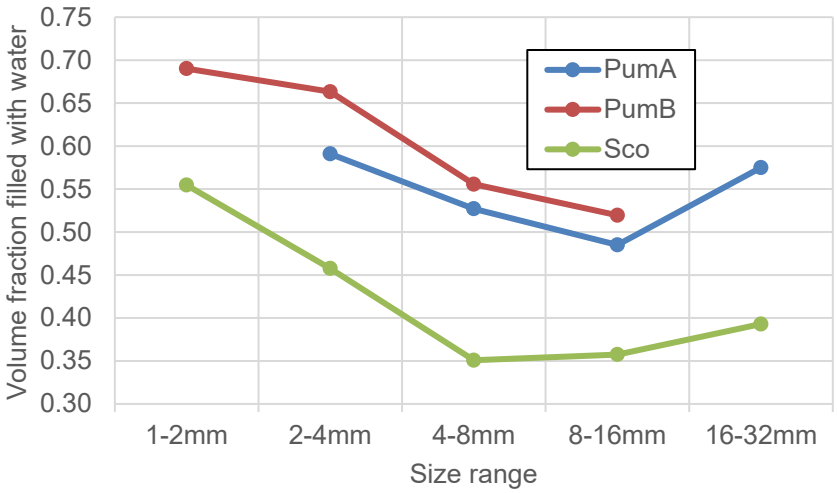

Figure 18: Volume fraction of container filled with water

Each of the two supplementary experiments show minor changes. The long-term absorption test, in which 500 mL of 8-16 mm *PumA* samples are placed in a beaker filled to the 1000 mL mark with water, covered, and left for 21 days, results in a net system volume decrease of 20 mL. The long-term evaporation test, with a covered 1000

mL beaker monitored over five days, shows no observable change in volume, suggesting that water loss via evaporation in similar experiments would be minimal.

The restrained immersion tool designed to keep pumices from floating on top of the water works as intended. Measurements of the tool's mass taken before and after immersion show that between 0.8-3.9g of water is absorbed by the wooden dowel during the period of immersion. This amount is considered when calculating the amount of water absorbed by the pumice and scoria.

Small mass decreases are observed in the clasts when dried after immersion. These mass decreases are assumed to be a result of abrasion creating dust which was then washed away with the tap water.

Comparing Distilled Water, Tap Water, and Graywater

Pure distilled water has pH 6.28 and is measured to have zero turbidity, TDS, or nutrient content. Tap water from the faucet in the lab (Eugene, OR) shows a pH of 8.85, turbidity of 1.4 NTU, TDS 34 ppm, and 0 ppm nutrient content. Graywater created for this project measures a pH of 7.23, turbidity of 43.7 NTU, TDS of 59, and nutrient content of 60. All three samples measured contain 0 measured EC units of conductivity. Comparing the pH values shows that the household products added to tap water in the creation of the graywater made the tap water more acidic, more turbid, and containing more dissolved solids and nutrients. See Figure 19 and Table 5.

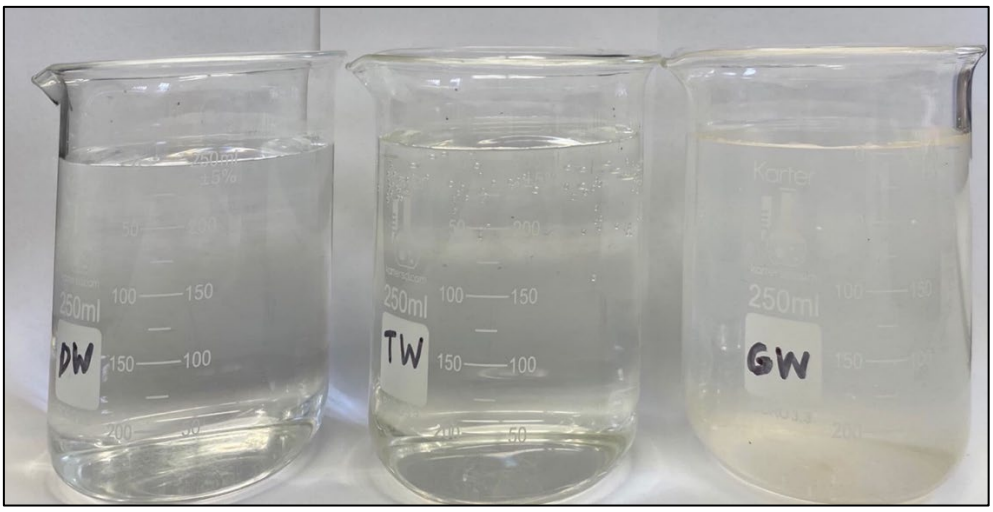

Figure 19: Three 250 mL beakers comparing distilled water ("DW"), tap water ("TW"), and graywater ("GW").

Note the increasing clarity from left to right. See Table 5 for detailed information on the turbidity values for each sample.

Table 5: Water quality comparison between distilled, tap, and graywater.

	Distilled water	Tap water	Graywater
pH	6.28	8.85	7.23
Turbidity (NTU)	-0.07	1.4	43.7
TDS (ppm)	0	34	59
Nutrient (ppm)	0	0	60
Conductivity (EC)	0	0	0

Static Graywater Absorption

Noticeable changes in the characteristics of the graywater are observed for all size fractions and all three sample types: turbidity and pH decrease with time, whereas TDS increases. Figures 20-28 show temporal changes in pH, turbidity, and TDS by sample type and for each size fraction. Figures 29-32 compare net changes (i.e., after a week of experiment) in turbidity, pH, TDS, and nutrients by size fraction for each sample type. Also included in these plots are measurements of the "control" graywater, which was not in contact with rock samples.

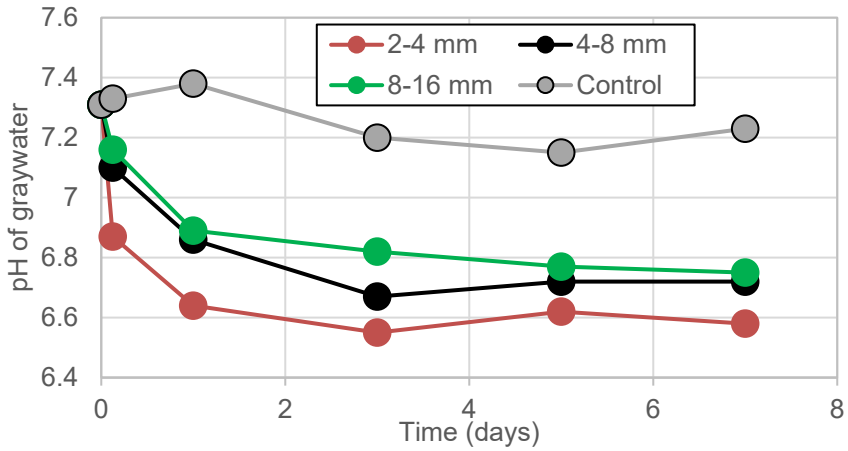

Figure 20: Graywater pH change with time in *PumA*

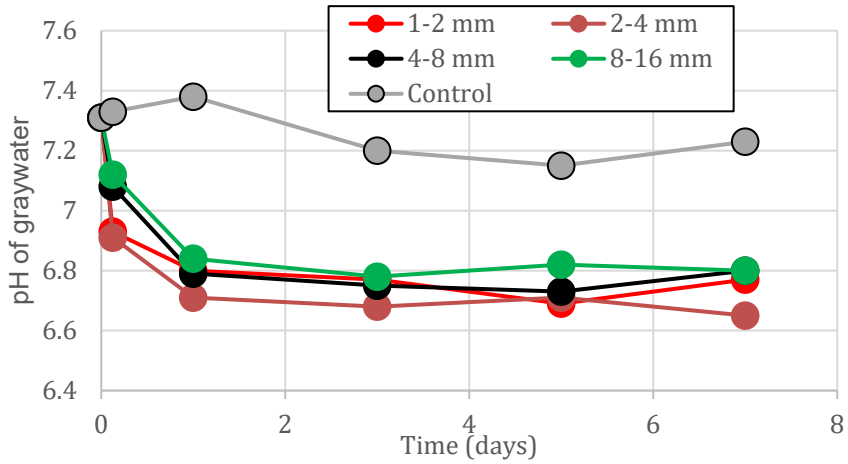

Figure 21: Graywater pH change with time in *PumB*

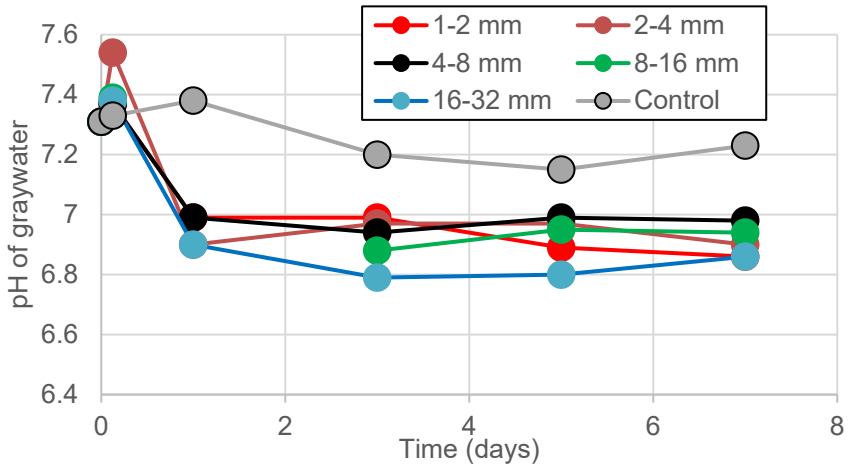

Figure 22: Graywater pH change with time in *Sco*

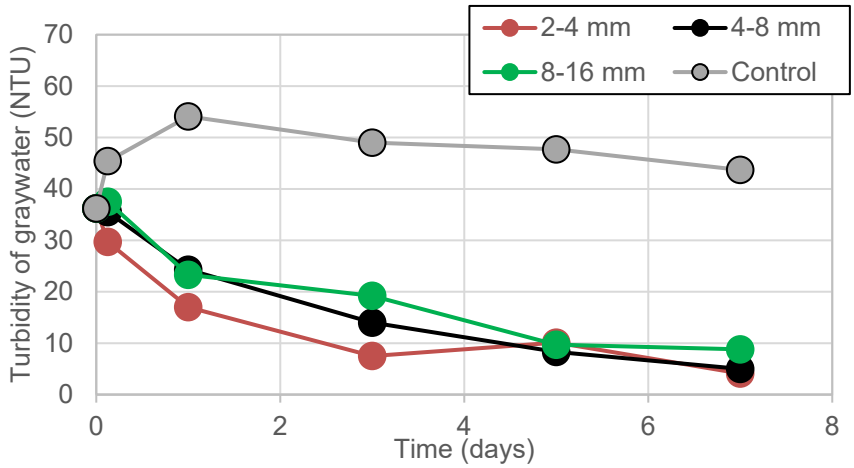

Figure 23: Graywater turbidity change with time in *PumA*.

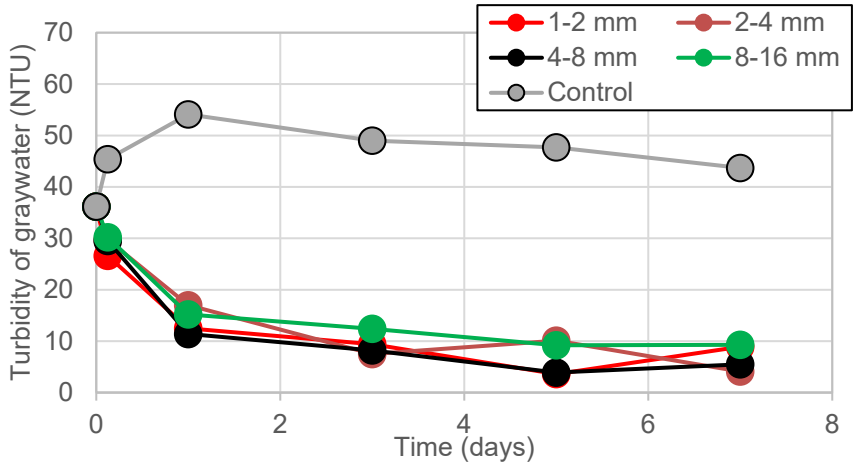

Figure 24: Graywater turbidity change with time in *PumB*.

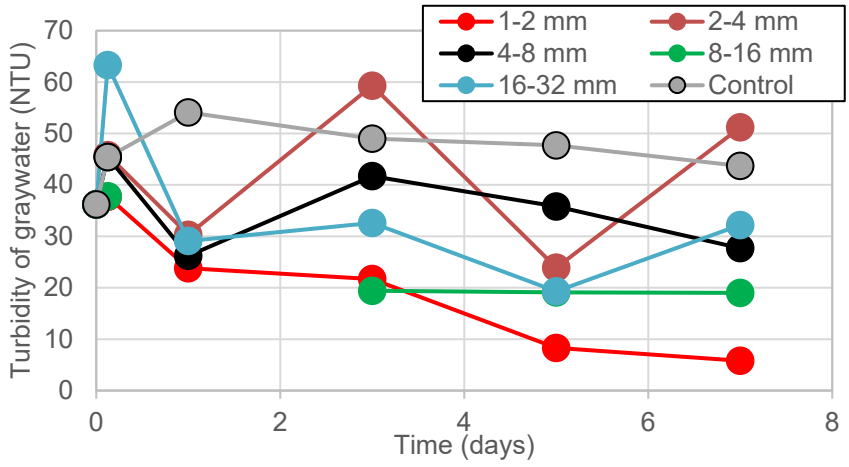

Figure 25: Graywater turbidity change with time in *Sco*.

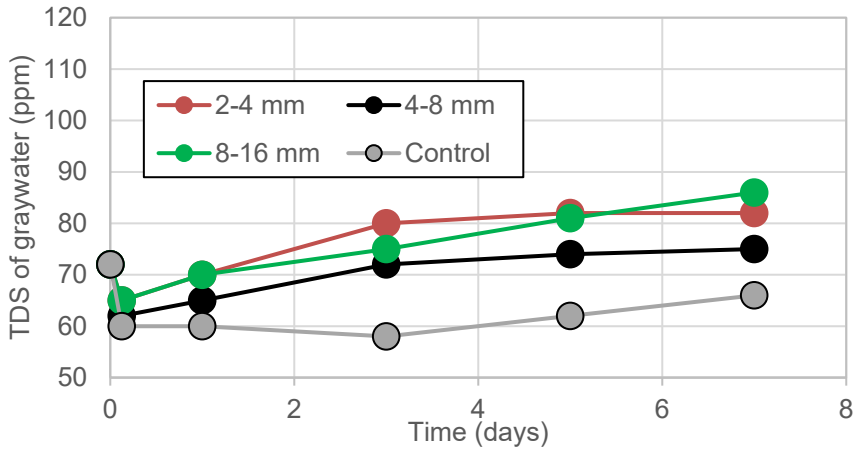

Figure 26: Graywater TDS change with time in *PumA*.

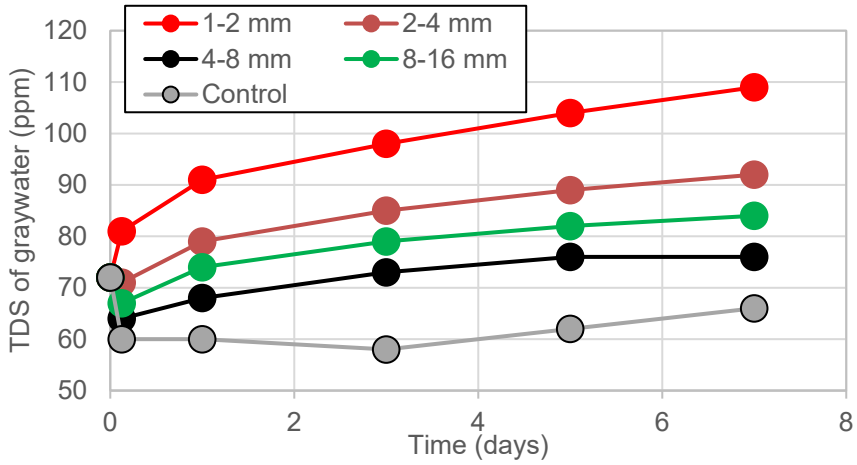

Figure 27: Graywater TDS change with time in *PumB*.

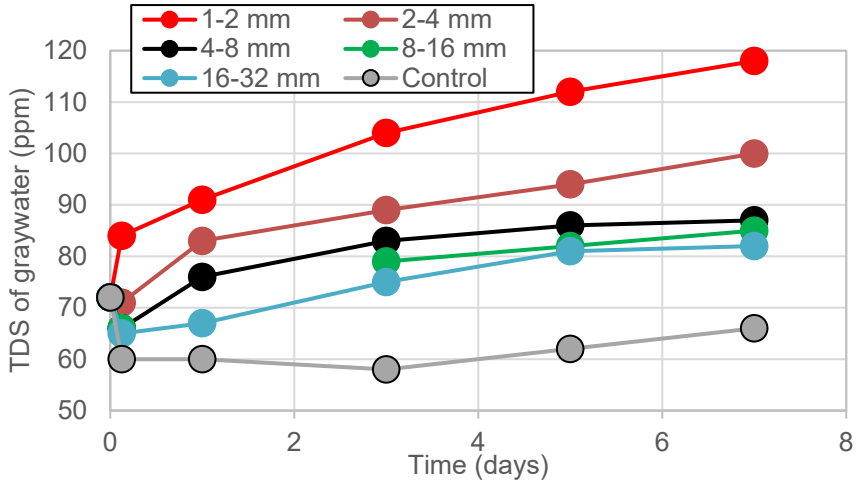

Figure 28: Graywater TDS change with time in *Sco*.

As seen in Figures 20-22, the change in pH is relatively similar across samples and size fractions. It consists in a rapid decrease of 0.3-0.6 unit during the first day (with the highest rate of decrease within the first 1-3 hours), followed by an overall plateau. At the end of the experiments, the total decrease in pH in the pumice (0.51-0.73 pH unit) is more significant than in the scoria (0.33-0.45 pH unit, see Figure 29). In the pumice, the decrease in pH is also slightly more rapid and overall, more important for small particles (1-2 mm and 2-4 mm) than for coarser ones (>4 mm), whereas this observation is less evident in the scoria sample, with slightly more variations between size fractions. Note that over the 7-day observation period, there is minor fluctuation of the control-graywater pH, resulting in a net change of less than 0.1, much less than the change observed in the rock-water experiments. Also recall that the pH of the original tap water was 8.85, and that once the influent particles of shampoo, soap, and other components were added, the resultant graywater had a pH around 7.23. Throughout the progression of this experiment, even as turbidity decreases and the water becomes visibly clearer, its pH continues to become more acidic than before.

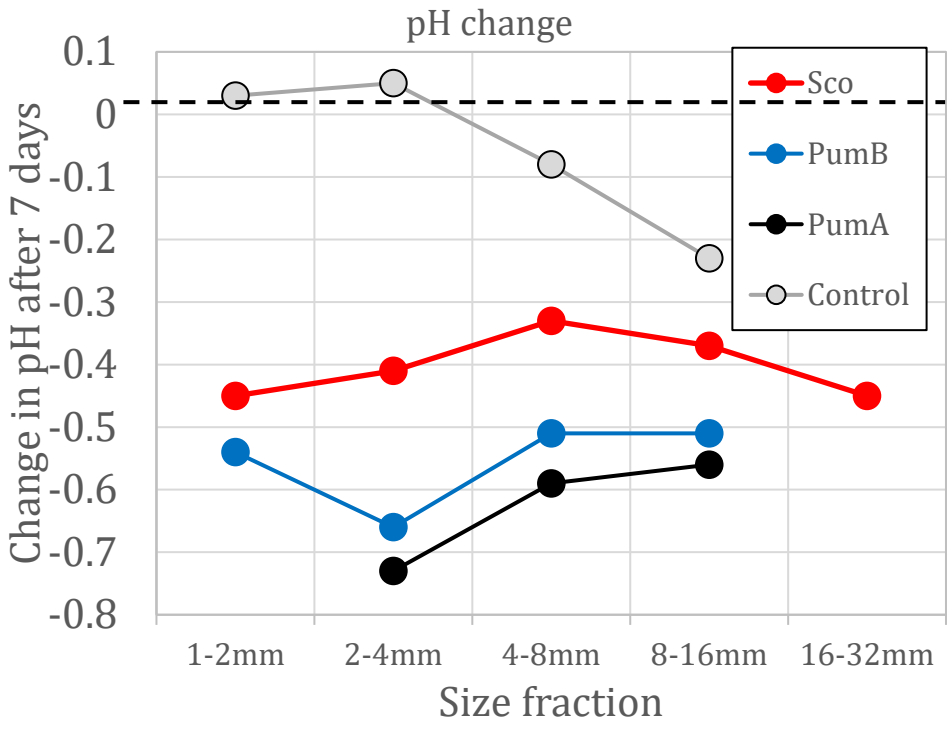

Figure 29: Net graywater pH change

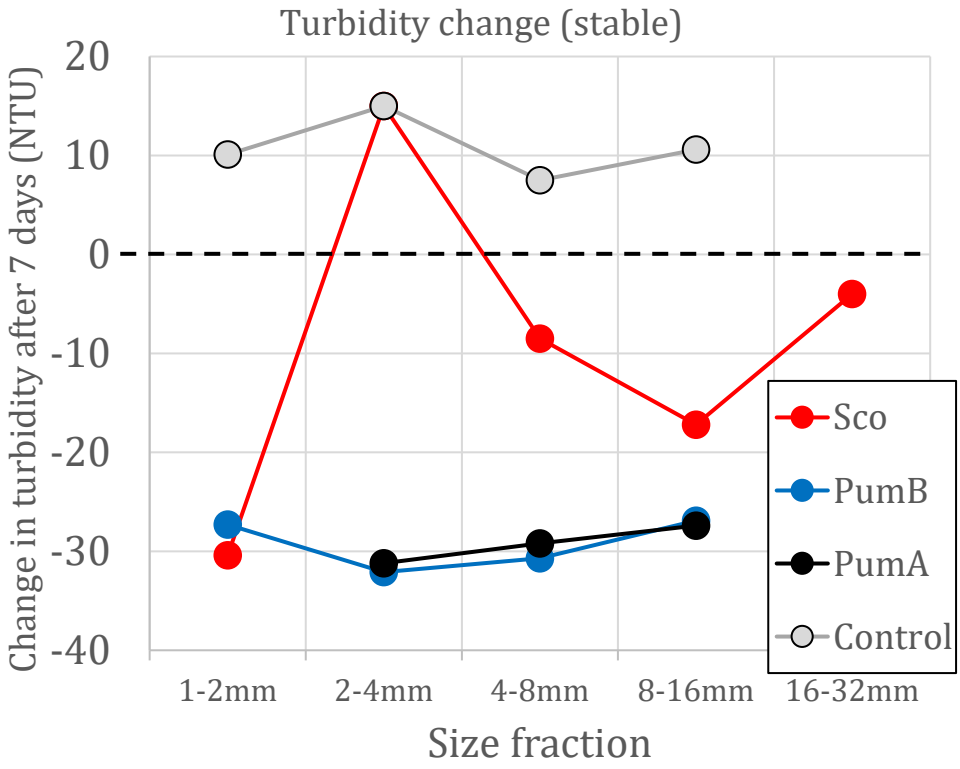

Figure 30: Net graywater turbidity change

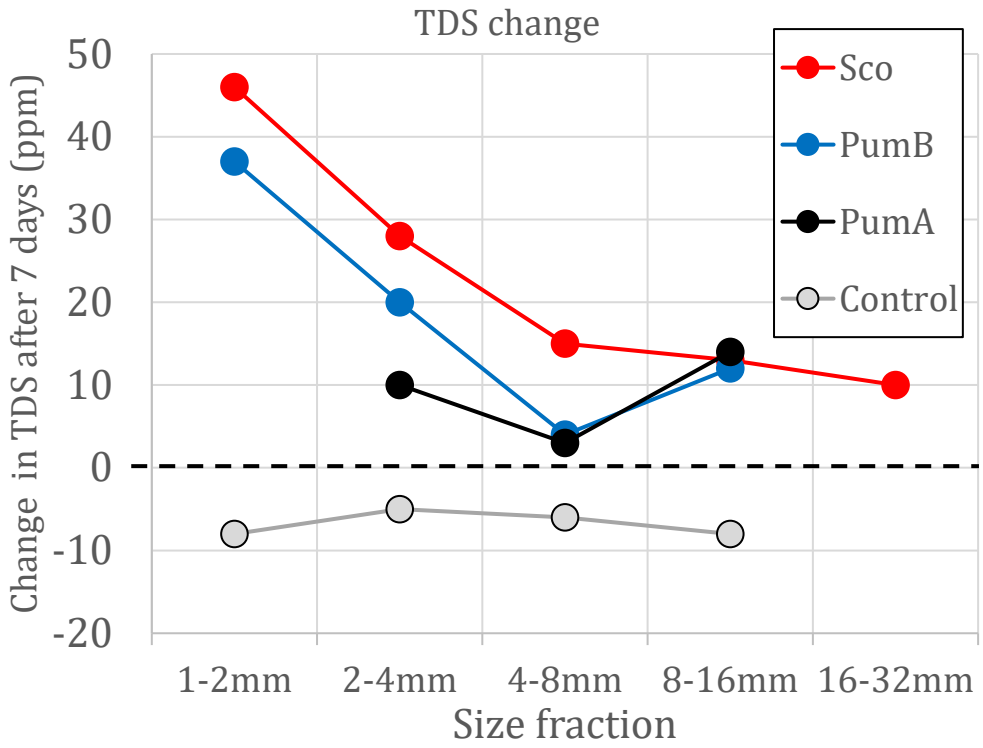

Figure 31: Net graywater TDS change

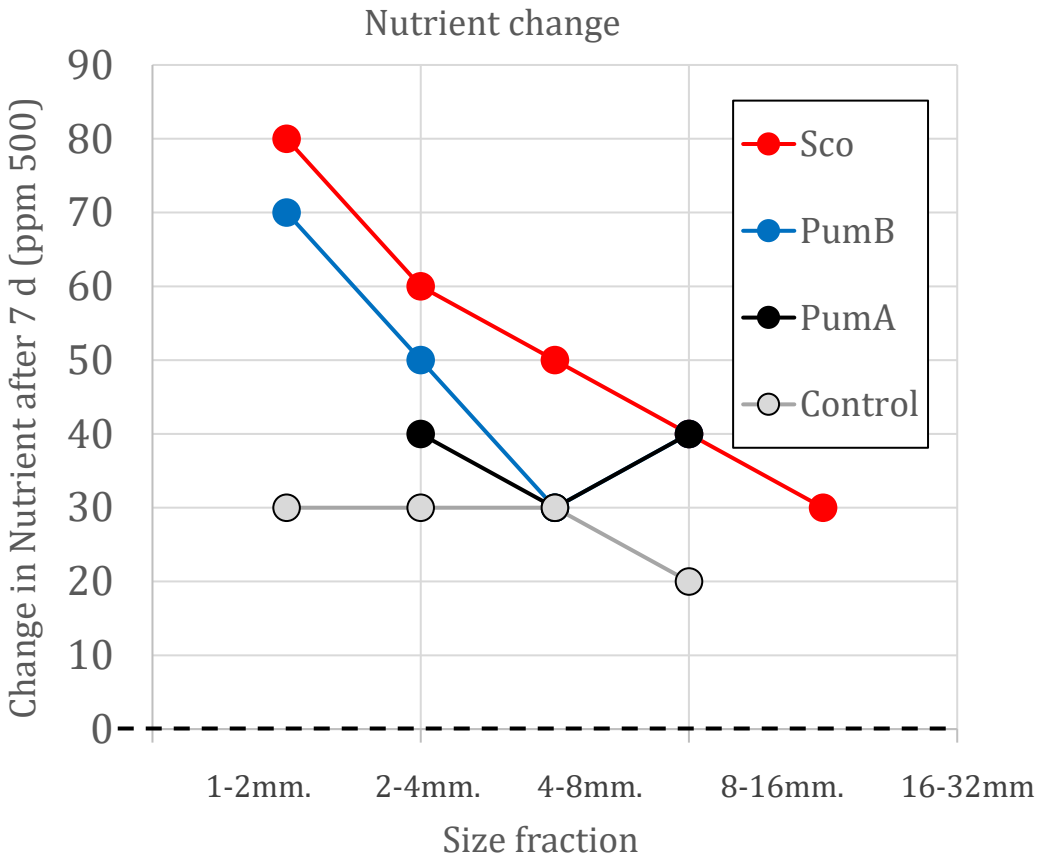

Figure 32: Net graywater nutrient content change

In both pumices and at all sizes, turbidity markedly drops with time (decrease of 26- 32 NTU in total), with the highest drop happening within the first day of the experiment (see Figures 23-25). The decrease in turbidity with time is different than the change in the control graywater experiment, in which turbidity increases by ~10 NTU in total over a week of experiment.

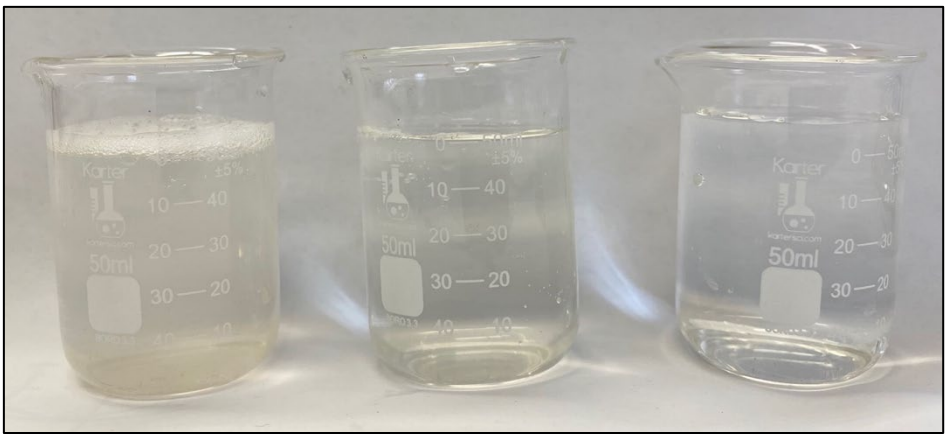

Figure 33: Three 50 mL beakers containing (left to right) control-batch graywater, identically created graywater after 7 days of immersion in *PumB* 4-8mm samples, and tap water. The control graywater (left) had a recorded pH of 7.23, turbidity of 43.7 NTU, and TDS of 66 ppm; the graywater after 7 days in the *PumB* 4-8 mm samples (middle) had pH of 6.8, turbidity of 5.5 NTU, and TDS of 76 ppm; the tap water (right) had pH 7.67, TDS 31 ppm, and was not measured for turbidity.

In the scoria, the turbidity changes are much less cohesive between size fractions and through time; three size fractions (2-4 mm, 4-8 mm, and 16-32 mm) show both sizeable increases and decreases in turbidity with time, one (1-2 mm) a consistent decrease like what is observed in *PumB*, and another (8-16 mm) almost no change at all. Two of the scoria size fractions (2-4 mm and 16-32 mm) exhibit peak turbidity values above that measured in the control group at the same time, and the 2-4 mm size fraction showed a net increase in turbidity over the one-week experiment.

In contrast to pH and turbidity, TDS (Total Dissolved Solids) increase across all sample types and size fractions at the end of the experiments (Figures 26-28). This increase is higher in scoria (10-46 ppm) than in pumice (3-37 ppm). After a short drop in TDS observed in all experiments during the first few hours, almost all size fractions show an overall logarithmic increase in this parameter with time (see Figures 26-28). In *Sco* samples, there seems to be a negative relationship between the increase in TDS and

particle size, with TDS readings increasing consistently more for smaller particles. This pattern is also observed in the pumice samples, albeit not as consistently (see Figures 26-28). Although the control experiment with graywater only also shows a decrease in TDS during the first ~1 day and then an increase during the rest of the experiment, the control experiment exhibits a net decrease of TDS of 5-8 ppm.

Nutrient content (Figure 32) typically follows the same pattern as TDS– a constant increase with time, higher in smaller size fractions and relatively linear in slope. However, the Bluelab meter used only reports values rounded to multiples of ten, resulting in less precise measurements. Additionally, the meter manual and website do not give specific details as to the exact nutrients which the meter measures, further complicating our understanding of why TDS and nutrient content readings would change both consistently together and in opposite temporal patterns to pH and turbidity.

Of the water quality parameters measured, the least amount of change is observed for conductivity. However, conductivity values still show a trend: consistent increases from 0 to 0.1-0.2 EC units at the 3- or 5-day time intervals, which then remained stable until the conclusion of the experiment. This increase of 0.1-0.2 EC unit is observed in all rock-water experiments, whereas none of the four graywater control batches show any increase of conductivity after 7 days. The low precision of the BlueLab conductivity pen used in this project prevent more precise quantification of conductivity change. In future projects, instruments with higher sensitivities will be used to obtain more detailed readings, so that the relationships between parameters can be better characterized.

Although temperature is monitored in these experiments, temperature changes only seem to vary based on the lab environment (the room in which the experiments were conducted is not temperature-controlled). The observed changes in graywater characteristics are thus thought to have occurred independently of temperature fluctuation.

Increases in water clarity in most samples become apparent by the 1-day or 3-day intervals; this is in line with the recorded rapid decrease in turbidity (an optical measure) observed in the first three days of the experiment. After the conclusion of the experiments, when the saturated clasts are removed from the graywater, they distinctly smell like soap and cleaning products (components of the graywater). These observations (of water becoming clearer and of clasts gaining a soapy odor) are consistent with the idea that suspended particles within the graywater are extracted by the rock particles and deposited within or on the clasts themselves, thus decreasing the water turbidity.

Further, in the scoria experiments for size fractions above 4-8 mm, the graywater poured out of the cylinders at the end of the experiments has a distinctive pale red coloration. When this graywater is poured into beakers to be measured, pieces of scoria dust visibly settle on the bottom of the beaker within seconds of being stirred. This suggests that fine material from the scoria is dislodged by and then incorporated into the graywater. This addition of suspended material in the graywater could bias turbidity measurements– turbidity values measured in the scoria experiments are inconsistent between size fractions and markedly different than the pumice samples. See Figures 32 and 33 for photographs of this observation.

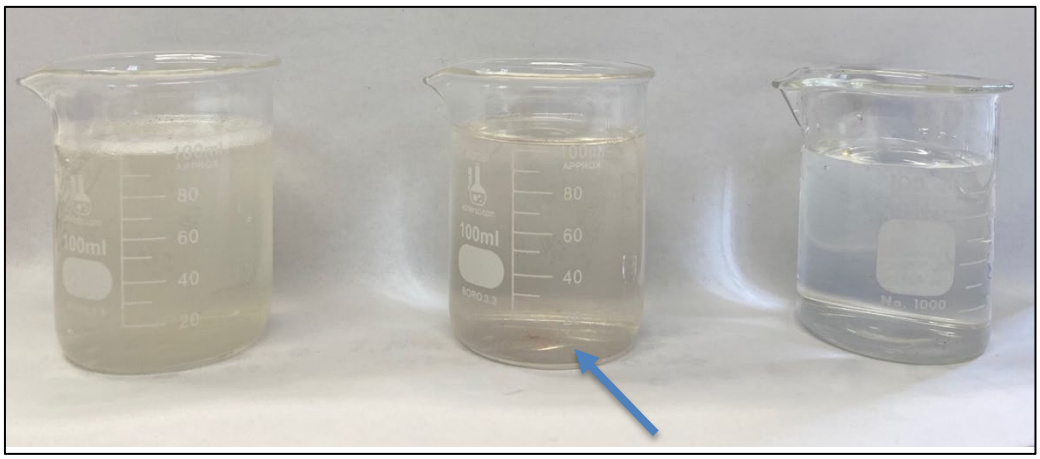

Figure 34: Three 100 mL beakers containing (left to right) control graywater, graywater after 7 days in *Sco* 16-32 mm samples, and tap water.

The control graywater (turbidity 46.8 NTU) has a soapy foam on top. In the center, the effluent water (turbidity 32.2 NTU) has a slight red coloration, and red dust-sized scoria particles are settling at the bottom of the beaker seconds after being stirred (indicated by blue arrow).

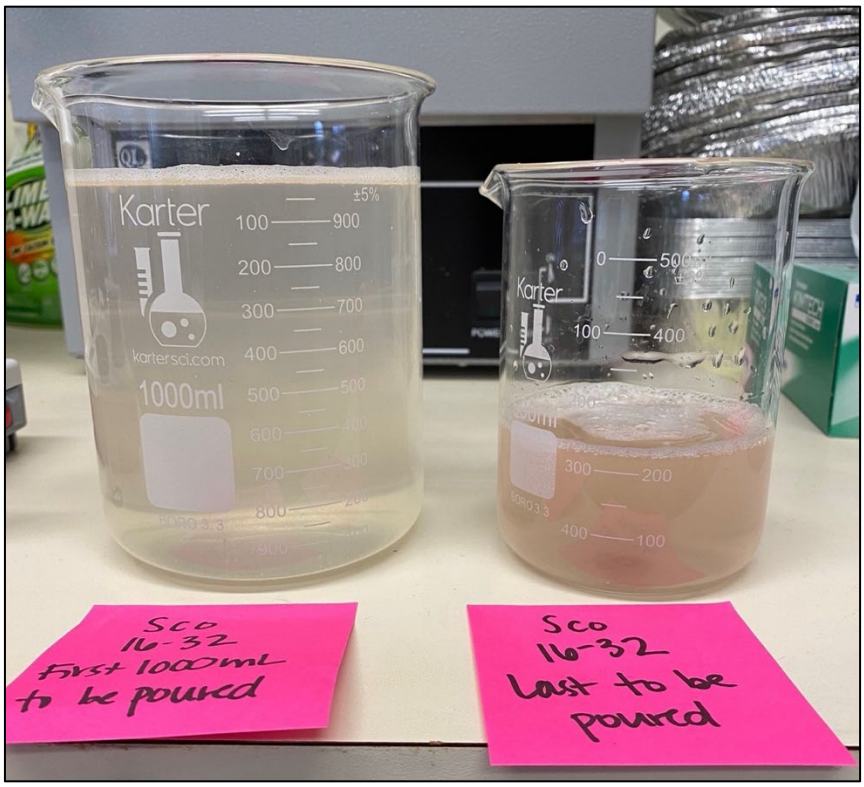

Figure 35: Two beakers showing changes in effluent between water at top and bottom of graduated cylinder from one hour of immersion in 16-32 mm *Sco*.

The water in the larger beaker, on the left, is water that first exited the graduated cylinder when the cylinder was emptied to take water quality measurements. The water on the right was the last graywater to drain from the cylinder, and visibly contains a high concentration of scoria particles (both large, settling on the bottom, and small, still in suspension) creating a dark red coloration.

A the initial addition of graywater to the samples, foam seeming to be composed of soap bubbles is noticed on the water surface of all cylinders. This foam is not observed when measurements are taken at the 3-day mark, or at any intervals afterward. Occasionally, during removal and measurement of graywater, thin plastic red fibers (no more than a few cm in length) are found in the water or on the rocks. These fibers are almost certainly from the lid of the red plastic bucket in which the graywater was stored and are not thought to have had any impact on the componentry of the graywater. Due

to limited supply of graduated cylinders, the static graywater absorption experiment was not conducted for the 16-32 mm size fraction of *PumA* samples.

Across all samples and size fractions, dry mass of test batches after graywater immersion showed minimal decreases– between 0.1 and 0.5 g lost per size fraction.

Discussion

The graywater immersion experiments in this project demonstrate a marked effect of the pumices and scoriae on water quality parameters. Despite minor variations in results between sample types and sizes, and between different rates and magnitudes of change, parameters generally are consistent, allowing for important conclusions to be drawn.

Although an overall decrease was observed in the dry mass of the pumice and scoria samples, this does not mean that no graywater ingredient particles were absorbed into clast structures. Firstly, mass decreases in the tap water experiments established that because of abrasion and dust loss it is typical for test batches to lose mass in a prolonged immersion experiment. Secondly, because graywater is produced using large amounts of water (consider how much water versus how much toothpaste is used to brush one's teeth, or how much shampoo is used in the shower), the recipe used to create this project's graywater used only small amounts of ingredients. In total (see Table 1), only 12.1 grams of material was added to 10 liters of tap water; this means that there are only 1.21 grams of "contaminant" mass per liter. Most of the graduated-cylinder-and-rock systems did not even use this much graywater– only the 16-32 mm scoria samples were in contact with more than one liter. Even if every gram of contaminant in the graywater was absorbed by this test batch, and even if those rocks lost zero mass due to abrasion, they would only gain 1.88 grams of mass– 0.15% of their total initial test batch mass (Table 4).

Inherently, the design and protocol of the graywater immersion experiments means that the setting is not truly "static"– each time sampling is required, the water is

forced to run through the column of rocks twice as it is poured out of and back into the graduated cylinder. This moment, in which the graywater percolates through a plane of clasts, is thus essentially a miniature filtration setting. Moving forward, it is important to consider that the results obtained in this experiment are the products of a combination of static and active interactions between rocks and graywater, and can give insight into details of both test settings.

In the graywater experiments, it is observed that pH and turbidity decrease rapidly in the initial 24 hours of immersion. During this time interval, samples are taken three times (at one, three, and twenty-four hours), each instance of which, as described above, results in more filtration. The rapid drop and subsequent stabilization in pH and turbidity suggest that the processes resulting in these phenomena either are dependent on the frequency of filtration events and plateau after a certain number of them or are dependent on time length of immersion and plateau at a time between the 1-day and 3-day measurements. Results from the tap water immersion experiments demonstrate that the majority of absorption of water into clast structures occurs immediately upon contact of rock and water; it is thus also possible that, with this rock-water contact occurring at multiple sampling intervals in the first 24 hours, by the 1-day mark, the graywater had entered all the pore spaces it could, leading to a plateau in pH and turbidity. This would imply that the changes in those parameters are thus connected to processes occurring as graywater enters and interacts with clasts– something which is more frequent in the first 24 hours of the experiment.

As opposed to pH and turbidity, which rapidly decrease and then plateau, total dissolved solids readings initially drop and then gradually increase throughout the 7-day

experimental period. This trend implies that the gain in TDS is a product of the amount of time for which the experiment is conducted. It remains unclear whether, if the system was left undrained for longer than seven days, if TDS would continue to increase with time or if a threshold would be reached and readings would plateau. This observed trend in TDS suggests that, during the length of the experiment, there is a reaction progressing with time resulting in a higher amount of dissolved solids in the graywater. It is possible that this is a chemical reaction between the surface of the rocks and the water; this is supported by the fact that, generally, TDS increases more in smaller size fractions (particularly so in *Sco* samples)– fractions which contain more surface area and contain more water by volume than larger sizes (Figures 26-28 & 31). It is also possible that, over the time of the experiment, suspended particles are being dissolved into the graywater, leading to the observed decrease in turbidity and increase in TDS. TDS is observed to increase in the control graywater, which is not in contact with rocks. However, it is not impossible that the control graywater came into contact with some rock material, because the experiments were conducted in a volcanology lab which does many experiments with pumice; surfaces in the lab accumulate pumice dust over time and the graduated cylinders used to hold the control samples could have been contaminated with pumice dust either before or during the experiments.

In weighing the possibility of a reaction occurring between the rocks' surfaces and the graywater, it is valuable to reconsider the observed changes in the sample mass and the precedent of rock abrasion leading to dust creation. It could be that the TDS changes observed in the graywater are related to abraded dust and material on the exterior and pore surfaces of the rock being dissolved into the water.

The graywater used in this project was created using tap water. Table 3 shows the variations in the measured water quality parameters between pure distilled water, tap water, and the synthetic graywater. Notably, the tap water originally has a pH of 8.85, while the graywater created from it has a pH of 7.23– the addition of the influent particles to the tap water made it more acidic. Prior to the graywater immersion experiments, it was thus predicted that, if particles seemed to be removed from the graywater by the rocks, pH of the effluent would then increase and return toward a more basic state having the particles which made it more acidic removed. However, this is the opposite of what is observed. pH readings in graywater during and after the experiment drop to around 6.7-6.8, becoming in fact more acidic despite the apparent removal of particles as demonstrated by the corresponding drop in turbidity. Causes of this phenomenon are unclear. Experts in aquarium science and maintenance often use pumice to neutralize water, suggesting that simple immersion of these rocks in water can lead to pH buffering.

Despite the questions surrounding the interactions between rocks and water, some important conclusions can still be reached about the efficacy of the pumice and scoria as filtration material. Most noteworthy is the decrease in turbidity, one of the most important features of water quality. In these graywater experiments, it is observed that smaller pumices, with a higher surface area-to-volume ratio, create the largest changes in pH, turbidity, and TDS. They are the most effective reducers of turbidity and were shown in the tap water experiments to have the most proportional area of contact with the water in their container. However, these smaller samples also show the largest increases in TDS.

While the trends in pH, turbidity, and TDS are clear, more work needs to be done, particularly chemically, to understand more about the interactions between the rocks and graywater and the effect that those materials may have on water which is filtered using them. It remains to be seen what particles are being dissolved in the graywater and from what source, whether these same observed changes would occur in an active-flow system, whether similar results would be obtained with rocks of different ages, source locations, or chemical compositions, and which water quality parameters influence each other most strongly. It is important to understand these and other questions before forming broader assumptions about the safety, efficacy, and applicability of pumice and scoria as graywater filtration media.

Conclusions

Prolonged contact between graywater and pumice or scoria results in a stabilization of the water pH to values of 6.6-7.0 and, for the pumice, to a decrease in turbidity of 74-89% to values below 10 NTU. It also results in an increase in the total dissolved solid content of the graywater of 3-46 ppm. The most significant decrease in turbidity occurs for small pumices (1-2 mm), and we thus interpret them as the most effective filtration media. These samples are shown to have the highest surface area in contact with the water, and their high packing fraction (0.8) and open porosity (70%), allow them to provide the most available space for water-rock interactions (a container full of such 1-2-mm pumice particles can hold 70% of its volume in water). To better understand these interactions, a more detailed understanding of chemical composition and reactions between the rocks and the water is required. Overall, the high porosity and packing fraction of pumice and scoria, combined with a tortuous network of interconnected pores, result in these rock samples significantly changing the quality of graywater, suggesting that these materials may be effective filtration media. These conclusions also suggest that graywater recycling systems using pumice and scoria could be implemented in communities around the globe.

Future applications of this research

Results from these experiments are very promising and raise more detailed questions concerning the numerous interactions between a pumice or scoria filter and graywater. I will have the opportunity to tackle some of these questions as, following the completion of my bachelor's degree in December 2022, I will return to the University of Oregon Department of Earth Sciences as a master's student to continue this research with Drs. Giachetti and Polizzotto.

First, more work reviewing existing literature surrounding graywater filtration and the chemical properties of pumice, scoria, and graywater is needed to properly interpret existing data and gather new data. Specifically, many of the unanswered questions from my thesis pertain to the chemical interactions between graywater and rocks; learning more about the chemical compositions of the rocks used and the graywater synthetized, the possible chemical exchanges within the system and the analytical methods appropriate to characterize these exchanges will be indispensable to the understanding of water-rock interactions.

More in-depth research is also needed about the status of graywater composition and recycling programs in the local area (Eugene-Springfield, Oregon), the state, and the country, and the world to better replace this project in the context of the local, regional, and international state of water infrastructure. There was not sufficient time to explore this line of research in this project, but I intend to spend more time in my master's project learning about the methods and types of wastewater treatment in my

region and what is being done with graywater where I live, so that I can better understand the applicability of my research in communities around the world.

As part of my master's program, I also intend to conduct more interpretation of data collected during my undergraduate thesis project. Among this data are the images obtained using the Scanning Electron Microscope (SEM) in the University of Oregon Knight Campus (Figure 8). A wealth of knowledge about the interior structure of my pumice and scoria samples can be derived from these images. Specifically, I hope to do pore size and shape distribution analyses to help form interpretations about the way the internal vesicle network of my samples influence filtration. Further, I intend to have thin sections made for the *PumB* samples and for *Sco* 1-2 mm samples, since the only thin sections that were made for this project were of *PumA* and *Sco* 2-32 mm samples. I would like to supplement these SEM images with 3-dimensional scans and analyses of clasts and filtration columns in the hope of finding which areas of the filter system and the clasts accumulate particles from graywater, and how that varies with sample type and size.

In tandem with this visual-spatial data, I intend to design and implement an active-flow graywater filtration system using pumice or scoria sourced from the same or similar locations as my undergraduate thesis samples. This system will include flowing, cycling water and frequent water quality testing to quantify changes in pH, turbidity, and TDS. Changes observed from this project's graywater immersion procedure conducted here will thus be compared to results from a more dynamic flow setting.

Along with these new active-flow experiments, I will also re-design the immersion experiments used in this project and conduct them again. These redesigned

procedures will explore physical and chemical interactions not yet investigated. They will include: the significance of system water pressure in absorption; the conditions affecting water saturation of clasts; changes in water quality of effluent tap water from immersion; and the effect of prolonging the time of rock-water contact. Quantifying these and other parameters about static immersion interactions between water and clasts will contribute to a better understanding of the interactions observed in the active flow experiments and in filtration settings in the real world.

Both the new active-flow and the redesigned immersion experiments will each contain a more detailed focus on chemical interactions between the rocks and the water. In combination with the more thorough literature review of aqueous chemistry, these experiments will include a wider variety of and more precise water quality-measuring instruments, more data frequent collection of chemical changes in water and rock samples, testing variations in graywater composition, and analyses of chemical and physical data from prior experiments. These experiments can also be redone using other rock samples in order to compare results between rocks of varying ages (and, thus, degrees of weathering), porosity and pore-network characteristics, and chemical compositions.

Incorporating these multiple new lines of work (extensive literature review, SEM imaging, and chemistry-focused active flow and immersion experiments) will ultimately allow me to generate a broader picture of the interactions occurring during graywater filtration with pumice and scoria. This knowledge could then be used to inform real-world graywater filtration systems. Data from this thesis and from future work can be combined to investigate filter system lifespans, cleaning methods, and the

degree to which these systems could be implemented on local, regional, or worldwide scales. As the global conditions creating water shortages and water quality issues continue to worsen, this work will become even more relevant and meaningful both to fellow wastewater and environmental researchers and to communities across the world in need of water recycling technologies.

Literature Review

The subject of graywater recycling exists at the intersection between a multitude of academic and social disciplines. Sources investigating aqueous geochemistry, landscape architecture, regional volcanology, wastewater treatment, and material science are often combined as bases for further research in the field of graywater recycling itself. This composite nature means that the bank of international literature relevant to graywater recycling projects is both broad and diverse, and incorporates a complex array of methods, precedents, and disciplinary approaches to research. In this literature review I summarize the main categories of sources relevant to my work, discuss the motivations of research in my field, and establish the place of my thesis adjacent to the literature it draws from.

Main categories of literature relevant to my research

Though the field of graywater recycling is much larger than my individual research, five general areas of literature are relevant to my specific thesis project.

I. Geological discussions of volcanic pyroclasts and Oregon rocks

Though not connected to wastewater recycling or graywater, geological analyses of pyroclastic deposits and volcanic eruptive histories are closely related to my individual research. With sample characterization and absorption experiments, my thesis project establishes a foundation for future analyses of flow interactions between graywater and the pumice or scoria filtering it. My specific work performs experiments and uses geoscientific instruments to constrain physical characteristics of pyroclastic samples. As such, to conduct my research I need a deep understanding of the processes

which form pumices and scoriae, baseline averages of porosity and pore distribution, and any place-specific factors which are related to the creation, deposition, or composition of the specific samples I am using.

For these reasons, it is beneficial for me to read extensively in the literature surrounding the volcanic products of both Mount Mazama, the large volcano whose massive eruption 7,700 years ago created Crater Lake (pumices), and the cinder cones near La Pine (scoriae). Reading literature such as the Bacon (1983) summary of the eruptive history of Mount Mazama provides geological context for my samples, allowing me to understand the composition of the rocks, the stages of eruption in which my samples were produced, and the role they play in the geologic history of their origin. Klug, et al. (2002) also discuss Mount Mazama, stating porosity measurements of Crater Lake pumices and using said porosity measurement to form conclusions about eruptive conditions.

Houghton and Wilson (1989) and Shea, et al. (2010) both discuss porosity in volcanic rocks including pumice and scoria. Houghton and Wilson create an index of vesicularity comparing pyroclastic deposits from both dry and wet magmas of varying chemical compositions; Shea, et al. advocate for a program they created (called FOAMS) to describe and image vesicles in a range of rock types and stages. Each of these papers shed light on the process of volcanic rock analysis, including what data is included and the technology involved in creating images depicting vesicles. In following research, more investigation is needed into the chemical composition of Mount Mazama pumice and scoria clasts, since the chemical interactions between the rocks and the pumices come under scrutiny following the results of my project.

II. Graywater componentry and output analyses

Many studies in the field of graywater research investigate graywater outputs or components at specific locations or in certain regions. One example, from 2013, published by Abedin, et al., characterizes the wastewater produced from several households in Dhaka City, the capital of Bangladesh. Abedin, et al. found that more than two-thirds of the average home's wastewater was graywater which had the potential to be reused if it was properly treated. The authors then argued that, as the rapidly-growing Dhaka City has increasingly struggled with water pollution and water shortages, technologies and systems to recycle graywater would greatly benefit the city and the country as a whole. This is common in studies which analyze graywater outputs and contents– many, like Abedin, et al., find that most domestic wastewater is actually reusable, and posit that systems or structures which recycle graywater would create positive change and alleviate existing water and resource stress.

do Couto, et al., in 2013 also conduct a place-specific graywater analysis. This paper analyzes graywater production and potable water use at airports in Brazil, finding that the average airport studied consumes comparable amounts of potable water to sizable human towns. Like Abedin, et al., the authors argued that graywater recycling would significantly reduce the airports' consumption of potable water, and listed several possible uses at airports for recycled but non-potable graywater: air cooling systems, irrigation of landscaping, aircraft and vehicle washing, and fire control testing.

Hafiza, et al. (2019) examine and characterize both graywater and blackwater produced in Jakarta, Indonesia. They find that bathing wastewater (specifically from showers) is the largest contributor to graywater content by volume, and briefly discuss

the lacking capacity of Jakarta's water treatment system to handle domestic outputs of wastewater (the water treatment system has a maximum processing capacity of only 25% of total wastewater output. The authors also analyze the pollutant loads of varying blackwater and graywater input sources and calculated the pollution in Indonesian watersheds resulting from discharge of these contaminated waters into ecosystems.

Further characterizations of urban graywater output are done by Katukiza, et al. (2015), studying wastewater in urban Uganda, and Oteng-Peprah, et al., doing the same in Ghana. Katukiza, et al. analyze graywater output from ten homes in a high population density urban area, quantifying both the proportion of graywater in wastewater (85%) and the chemical oxygen demand (COD) of graywater generated by different sources. Oteng-Peprah, et al. (Jan. 2018) analyze household graywater outputs in comparison to other wastewater sources, also tracking COD as well as BOD (biological oxygen demand), nutrient levels, and salinity.

Understanding the componentry of graywater is crucial to its effective filtration. Future applications of my research may include the implementation of volcanic rock graywater recycling systems in places besides the United States; as such, it is important to evaluate trends and variations in graywater between different communities and countries worldwide. These sources, from Bangladesh, Brazil, Indonesia, Uganda, and Ghana both demonstrate variability in graywater componentry and highlight consistencies throughout different continents and levels of socioeconomic development.

III. Documents listing qualitative graywater regulations, standards, and recipes

To determine if the graywater in volcanic rock filtration experiments is usable after the filtration process, one must use established standards to judge the achieved

efficacy. Some documents, often published by government agencies or water-regulating bodies, offer parameters to define “clean” or “healthy” water based on established thresholds for contamination and chemical composition. In addition to this, organizations like the National Science Foundation (NSF) have created standards for what makes up graywater, so that projects like mine can create and test synthetic graywater with consistent levels of specific components and particles. Using water quality instruments and information from both of these source types (water quality standards and graywater component classifications), my project can precisely judge the amount of particles removed by its system and exactly how “safe” or “clean” the recycled graywater is, thus illuminating the potential for both graywater reuse and the application of said system in the real world.

The graywater used in my project was created with a simplified graywater recipe provided in personal communication by Markus Koeneke, a researcher working on a graywater filtration project associated with the University of Oregon. This recipe lists materials for a graywater mixture which is created synthetically, and not collected from actual domestic output sources. Using this simplified recipe (without large particles like food or hair) allows for a baseline understanding of how more-complex graywater might interact in a similar system, and sets a foundation for further research and conclusions using real-life graywater.

A more in-depth review of the state of graywater and other wastewater recycling in the Eugene area will be beneficial, especially partnered with a comparison to other systems at the household, city, state, and national level in other places. This is an area which I plan on exploring in depth in my master’s project, partly through

communicating with representatives of the Metropolitan Wastewater Management Commission, the organization responsible for recycling wastewater in the Eugene-Springfield area. Further communication is also expected with Pat Heins, at the Oregon Department of Environmental Quality, with whom I met in April for a brief overview of the status of graywater recycling in the state of Oregon.

IV. Literature discussing developments in the field of graywater recycling

In the last few decades, the field of graywater reuse has expanded greatly. Sources from government agencies, academic publications, and nonprofit groups review graywater recycling systems and methods, compare their merits, and discuss their applicability to the global public. These range from graywaterAction.org, the website for a nonprofit organization aiming to connect interested citizens with home graywater reuse systems, to Eriksson and Eilersen's analysis of graywater sludge, a material which settles out of conventional graywater treatment systems and contains many of the contaminants and particles which are filtered out of the graywater. Some sources discuss risks associated with graywater reuse systems, such as Cook's 2016 paper reviewing graywater produced from different household sources in England and California, as well as the different uses and risks carried with "light" and "dark" graywater.

A sub-field of this area of literature is that discussing graywater recycling models which use materials, processes, and structures derived from the natural world rather than synthetically-created solutions. Boano, et al. (2020) provide an overview of varying methods of graywater recycling derived from natural processes– grouped under the term "nature-based solutions". These methods include constructed wetlands, green

walls, and green roofs as ways to filter graywater and return it for household use. The article also reviews the typical components of graywater, conventional methods for its treatment, and application of both nature-based and conventional technologies in real-world settings. Within the field of wastewater treatment, many view it as most effective, sustainable, and accessible to treat graywater with natural materials instead of with conventional chemical or mechanical treatments. The same sentiment is echoed in Mark Nelson's book "The Wastewater Gardener," which reviews ways for readers to incorporate their own home wastewater into productive gardens.

Many researchers and global organizations publish summaries of graywater treatment systems and literature relevant to the field. These include the Pacific Institute's overview of graywater systems and their relevance to sustainable water management (Allen, 2010) and information published by the University of New South Wales' Water Research Center (WRC), which serves as a hub for wastewater treatment and systems research (WRC, 2022). Specific instructions for constructed wetland filtration systems are distributed by the United Nations Human Settlements Programme, which in 2008 published a manual for creating constructed wetlands systems with a focus for their application in developing regions (UNHSP, 2008). Pinto, et al. (2021) examine trends in global graywater reuse, and Oteng-Peprah, et al. (Aug. 2018) review graywater characteristics and treatment systems in urban Ghana.

Systems which use unfiltered graywater for irrigation purposes are common and frequently-published. Examples include Laafat, et al. (2017), which studied the reuse of laundry graywater for irrigation in rural communities, and Misra, et al. (2010), which used laundry water to irrigate tomato plants. Although my project focuses on the

filtration of graywater, it is important to understand how graywater is already being used in unfiltered states in projects around the world.

V. Testing volcanic rocks as filtration media for contaminated water

Sources which specifically test volcanic rocks as filtration media for contaminated water are most relevant to my thesis project. Aregu, et al.'s studies from 2017, 2018, 2021, and 2022 focus on wastewater from tanneries, which emit water with high levels of hazardous pollutants, including heavy metals and chemical nutrients. The researchers tested the ability of pumice and scoria to filter these pollutants out of wastewater produced by tanneries in Ethiopia. Ultimately, using these volcanic media as filters proved to be effective: both pumice and scoria were more than 70% effective in their removal of chromium, sulfate, phosphate, and nitrate from the wastewater. These studies establish an important precedent: that, due to their porosity and associated high surface area, pumice and scoria can function as filters, removing suspended particles and chemical components from wide varieties of contaminated water.

Many other sources detail the use of volcanic rock media in filtering heavily-contaminated water. Some projects create real-world systems testing the filtration of actual contaminated water; these include Kelm (2003), filtering mineral-processing slurries, Aksay (2010), using olive-mill wastewater, and Li (2018), with heavy metal contaminated groundwater. Others instead create synthetically- contaminated water to test specific removal capabilities of filtration media, such as Asere (2017), testing arsenic removal, Kam (2011), testing mixed gas filtration, and Khorzughy (2015), testing cadmium removal.

Additionally, Farizoglu, et al., in 2003, conducted a study comparing the use of pumice and sand in bed filtration (a system in which the filtration media are contained in lateral beds, through which contaminated water is directed to flow through for filtration). Although pumice was found to effectively reduce turbidity due to its high porosity and correlated high surface area, these pores fill with filtered material over time, slowly decreasing the speed and efficacy of filtration. Overall, however, pumice beds were more than 10% more effective in decreasing turbidity in water than comparable sand beds.

Other important works using volcanic rock filtration include Kuslu (2013), which used sand- pumice-gravel filters, Heydari (2018), which compared raw and manganese-modified pumices in phenol filtration, Albalawneh (2017), which compared gravel filtration with volcanic tuff filtration, and Bilardi (2013), which discussed methods of improving iron-enriched pumice filtration systems.

The results of these studies seem to suggest that my experiments to filter graywater with pumice will show meaningful and successful results. Though only some of the research in this field is specific to graywater filtration, the principles of particle removal from contaminated water are the same: the more particles that are removed, the more effective the filtration medium. Under this parameter, research has shown pumice and scoria to be highly-effective filters, a fact my thesis research aims to support.

Research motivations in the field of graywater filtration

Much development in the field of graywater filtration is motivated by the ever-worsening climate crisis and the rapid growth of human population in developing areas, which are combining to create more frequent drought, greater consumption of = potable

water resources, and increasing amounts of pollution entering ecosystems. Considering these dire circumstances, which are harming health and causing unrest in communities around the world, methods for recycling wastewater are exceedingly needed and relevant. Works in the field of graywater reuse typically examine which filtration media function effectively as filters and why, as well as what graywater recycling systems might look like applied at different scales in houses, buildings, or entire communities. Since many of the places in which water crises are worsening are in developing regions, the systems which may be most effective are those which are easy to replicate, affordable, and made of materials which are easily accessible to many people. Much research has focused on creating or studying systems which fit these needs, so that health, quality of life, and future sustainability can be improved for communities in all parts of the world.

The place of my research in relation to its adjacent scholarly literature

Studies which test graywater filters, including pumice and scoria, typically frame their results in terms of filtration efficacy. Much research in this field is conducted with the intention to investigate how a filtration system composed of a certain material changes the amount of a certain contaminant or parameter in water. Products of studies like these typically are quantitative, listing results in terms of measured decreases of contaminants, and sometimes include information about possible applications or uses of these filtration systems in the real world.

In contrast, however, material efficacy is not the sole focus of my research. While the success of the pumice and scoria filtration is important, the bulk of my individual thesis project centers on investigating why observed water-rock interactions

and water quality changes occur. My current and upcoming work will future conclusions about interactions between graywater and pumice or scoria filtration media during flow, which may result in a better understanding of how pore location and size affect particle removal, how chemical reactions between rock and water occur, where water flows in relation to samples, and whether the samples erode significantly during flow. This is a unique approach in the field of volcanic rock graywater filtration.

Using this information about flow interactions, future research can gather a better understanding of why volcanic rock filtration systems work, how long they last, and how their attributes affect their potential incorporations into real-life communities in need of clean water. This applicability is another reason my research is unique in the field of wastewater recycling solutions: being created in a wide variety of volcanic events and settings, pumices and scoriae are widely available in locations around the world. This means that, with instructions on how to assemble filtration systems, methods from this research could be easily incorporated into wide varieties of cultures and communities.

Glossary

Abrasion: The process by which clasts rub against one another, grinding off small pieces of rock and creating dust.

Active flow: A setting in which fluid is moving (as opposed to a setting in which water is still).

Bed filter: A common method of wastewater filtration composed of a horizontal plane of particles which water flows through laterally; in this process of flow, particles from the influent are trapped on or inside the filter medium and are thus removed from flow.

Blackwater: Wastewater containing sewage (fecal matter), typically from toilets.

Cinder cone: A steep conical volcanic landform made of basaltic rock ejected around a vent.

Clast: A fragment or piece of rock. In this project, a "clast" could be any singular piece of pumice or scoria.

Effluent: Water that flows into a system (e.g. unfiltered graywater)

Felsic: Magma, lava, or cooled igneous rocks which have high contents of silica. Felsic lava is more viscous (stickier) than mafic lava, and felsic rocks are typically lighter in color than mafic ones.

Graywater: Non-sewage wastewater from uses like cleaning, washing, and cooling. Typical household graywater inputs include laundry and dishwashing machines, showers, and sinks.

Influent: Water flowing out of a system (e.g. filtered graywater).

Lithic: Also an adjective for an object pertaining to or consisting of rock, "lithics" can also refer to pieces of rock in sediments or samples. In this project, "lithics" are small pieces of obsidian or other volcanic rocks deposited at the same time as the pumice or scoria samples.

Mafic: Magma, lava, or cooled igneous rocks with lower contents of silica and higher proportions of heavier elements like magnesium and iron. Mafic lava is less viscous (runnier) than felsic lava, and mafic rocks are typically darker in color than felsic ones.

Packing fraction: In a container of particles, the proportion of container volume taken up by particles as opposed to void (space between particles).

Porosity: In a given particle, the amount of that particle's volume which is occupied by void space. (Note: in this project, "porosity" is used exclusively to discuss the average void fraction of individual pumice or scoria clasts; however, other fields of earth science use the term to discuss the void space present in a larger unit of soils or other sediments). Connected porosity is the volume fraction of void space in a particle which is connected to the outside environment and is often the result of multiple interconnected bubbles (see Figure 2). Isolated porosity represents the fraction of particle volume occupied by separate bubbles, pockets of gases or air which are surrounded on all sides by solid material and do not connect to the outside.

Pumice: A light, porous volcanic rock formed typically through felsic eruptive activity.

Pyroclast: A rock composed of volcanic material which was ejected during an eruption. Pyroclasts include porous materials, like pumice and scoria, as well as denser ones, like volcanic bombs or lapilli.

Scoria: A porous volcanic rock formed in mafic eruptive activity.

Solid phase: The material in a clast of pumice or scoria which is solid rock, not pore space/void. The walls surrounding the bubbles in these vesicular rocks are solid phase.

Static: Still, unmoving. “Static” experiments in this project are those in which water does not move relative to the rocks it surrounds.

Subduction: A tectonic setting in which two plates collide, with one plate sliding under the other. Subduction occurs at convergent boundaries between an oceanic plate (which subducts) and a continental plate (the “overriding” plate).

Tephra: Rocks and ash ejected during volcanic eruptions.

Uplift: The movement of an area of land surface relative to the land around it; typically occurs on large scales. Uplift can be typically caused by tectonic forces such as the sliding of one tectonic plate beneath another, volcanic forces such as intruding magma beneath the surface, or rebound, which is an upward-moving response of ground surface to the removal of overlying weight (like a couch cushion rising up after someone who was sitting stands up).

Vent: A place on the Earth’s surface where volcanic activity occurs, including the eruption of gases, lava, and/or tephra.

Vesicle: A pore, hole, or bubble in a rock.

Appendices

Appendix 1. Calculating physical characteristics using PartAn and Helium Pycnometer parameters

ρ_{sol} = density of solid phase rock $(\frac{g}{cm^3})$

V_{sol} = volume of solid phase rock (cm^3)

m = mass (g)

V_{ext} = external volume of rock (cm^3)

V_{con} = volume of connected pore space (cm^3)

V_{iso} = volume of isolated pore space (cm^3)

ϕ_{tot} = total porosity (volume fraction of void space) of rock

ϕ_{con} = total connected porosity (volume fraction of connected void space) of rock

ϕ_{iso} = total isolated porosity (volume fraction of isolated pore space) of rock

Using mass data from the balance, external volume data from the PartAn, and data from the helium pycnometer, I calculated density, porosity, and volume of void space for each of my samples. When solid samples are put in the helium pycnometer, the instrument calculates a value that is the combined volume of solid material plus isolated pores (1). By crushing those same samples and putting them in the pycnometer, the instrument gives the total volume of just the solid material (not including void). Solid-state density is calculated by dividing the sample mass by its solid state volume (2). The volume of isolated pores is found by subtracting the solid state volume from the total volume from the pycnometer (3). The volume of connected void space (4) is calculated using the summed volume from the pycnometer and the external volume as found by the PartAn. Total porosity is found using mass, density, and external volume

(Equation 5); connected and isolated porosity (Eqs. 6 and 7) are found the volumes of connected void and external space and the total porosity.

$$[V_{sol} + V_{iso}] \tag{1}$$

$$\rho_{sol} = \frac{m}{V_{sol}} \tag{2}$$

$$V_{iso} = [V_{sol} + V_{iso}] - V_{sol} \tag{3}$$

$$V_{con} = V_{ext} - [V_{sol} + V_{iso}] \tag{4}$$

$$\phi_{tot} = 1 - \frac{m}{\rho_{sol} \cdot V_{ext}} \tag{5}$$

$$\phi_{con} = \frac{V_{con}}{V_{ext}} \tag{6}$$

$$\phi_{iso} = \phi_{tot} - \phi_{con} \tag{7}$$

Appendix 2. Quantifying rock-water interactions from tap water immersion data

V_{avail} = volume of available void space in column of rock (cm^3)

X_{avail} = volume fraction of available void space in rock column

X_{occ} = fraction of rock column filled with water during immersion

m_{cl_t} = mass of water in clasts before drainage of graduated cylinder (g)

ϕ_{eff} = effective porosity (fraction of connected pore space filled with water during immersion)

Mass and volume data from the tap water immersion experiments, as well as previous porosity and packing fraction calculations, was used to find information about the spatial relationships between rocks and water. The volume of available void space (1) was found using connected pore space volume, the total volume of the given graduated cylinder, and packing fraction; the proportion of this space (2) was calculated with packing fraction and connected porosity. The mass of water saturated into clasts before being drained was found by combining the volume of water initially added to the system, the volume of water above the rock column when the experiment ended, packing fraction, and the total system volume (Equation 3). This number was used with the volume of available space to find "effective porosity" (4), the proportion of available void space which was actually filled with water at the end of immersion before being drained. Lastly, effective porosity and packing fraction were utilized to find the proportion of space in the graduated cylinder which was occupied by water at the end of immersion.

$$V_{avail} = V_{con} + (V_{tot} \cdot (1 - PF)) \tag{1}$$

$$X_{avail} = (PF \cdot \phi_{con}) + (1 - PF) \tag{2}$$

$$m_{cl_t} = V_{added} - V_{above} - ((1 - PF) \cdot (V_{tot})) \tag{3}$$

$$\phi_{eff} = \frac{m_{cl_t}}{V_{avail}} \tag{4}$$

$$X_{occ} = (1 - PF) + (PF \cdot \phi_{eff}) \tag{5}$$

Bibliography

Abedin, S. B., & Rakib, Z. B. (2013). Generation and Quality Analysis of Greywater at Dhaka City. Environmental Research, Engineering and Management, 64(2), 29–41. https://doi.org/10.5755/j01.erem.64.2.3992

Aksay, E. K., & Akar, A. (2010). The Filtration of Olive-Mill Wastewater with Pumice Ores. Fresenius Environmental Bulletin, 19(11A), 2672–2677.

Alatorre, B. (2021, April 29). *How Giiwas (Crater Lake) Came To Be*. Klamath Tribes News and Events.https://klamathtribes.org/news/crater-lake-giiwas-a-sacred-place-the-fulbright-event-recording-featuring-klamath-tribal-elders/.

Albalawneh, A., Chang, T.-K., & Alshawabkeh, H. (2017). Greywater treatment by granular filtration system using volcanic tuff and gravel media. Water Science and Technology, 75(10), 2331–2341. https://doi.org/10.2166/wst.2017.102

Allen, L, Christian-Smith, J., & Palaniappan, M. (2010). Overview of Greywater Reuse: The Potential of Greywater Systems to Aid Sustainable Water Management. Pacific Institute.

Aregu, M. (2017). Removal of Hazardous Pollutants from Tannery Wastewater by Naval Filter Medium (Pumice) Through Adsorption and Filtration Method. IOSR Journal of Environmental Science, Toxicology and Food Technology (IOSR-JESTFT), 11, 38–45. https://doi.org/10.9790/2402-1109023845

Aregu, M. B., Asfaw, S. L., & Khan, M. M. (2018). Identification of two low-cost and locally available filter media (pumice and scoria) for removal of hazardous pollutants from tannery wastewater. Environmental Systems Research, 7(1), 10. https://doi.org/10.1186/s40068-018-0112-2

Aregu, M. B., Asfaw, S. L., & Khan, M. M. (2021). Developing horizontal subsurface flow constructed wetland using pumice and Chrysopogon zizanioides for tannery wastewater treatment. Environmental Systems Research, 10(1), 33. https://doi.org/10.1186/s40068-021-00238-0

Aregu, Mekonnen Birhanie. “Industrial Wastewater Treatment Efficiency of Mixed Substrate (Pumice and Scoria) in Horizontal Subsurface Flow Constructed Wetland: Comparative Experimental Study Design.” *Air Soil and Water Research* 15 (January 2022): 11786221211063888. https://doi.org/10.1177/11786221211063888.

Asere, T. G., Mincke, S., De Clercq, J., Verbeken, K., Tessema, D. A., Fufa, F., Stevens, C. V., & Du Laing, G. (2017). Removal of Arsenic (V) from Aqueous Solutions Using Chitosan-Red Scoria and Chitosan-Pumice Blends. International Journal of Environmental Research and Public Health, 14(8), 895. https://doi.org/10.3390/ijerph14080895

Bacon, C. R., & Lanphere, M. A. (2006). Eruptive history and geochronology of Mount Mazama and the Crater Lake region, Oregon. Geological Society of America Bulletin, 118(11–12), 1331–1359. https://doi.org/10.1130/B25906.1

Bilardi, S., Calabro, P. S., Care, S., Moraci, N., & Noubactep, C. (2013). Improving the sustainability of granular iron/pumice systems for water treatment. Journal of Environmental Management, 121, 133–141. https://doi.org/10.1016/j.jenvman.2013.02.042

Boano, F., Caruso, A., Costamagna, E., Ridolfi, L., Fiore, S., Demichelis, F., Galv o, A., Pisoeiro, J., Rizzo, A., & Masi, F. (2020). A review of nature-based solutions for greywater treatment: Applications, hydraulic design, and environmental benefits. The Science of the Total Environment, 711, 134731–134731. https://doi.org/10.1016/j.scitotenv.2019.134731

Bosshard-Stadlin, Sonja A., Mattsson, Hannes B., Stewart, Carol, & Reusser, Eric. (2017). Leaching of lava and tephra from the Oldoinyo Lengai volcano (Tanzania): Remobilization of fluorine and other potentially toxic elements into surface waters of the Gregory Rift | Elsevier Enhanced Reader. *Journal of Volcanology and Geothermal Research*, *332*, 14–25. https://doi.org/10.1016/j.jvolgeores.2017.01.009

Brown, S. K., S. C. Loughlin, R.S.J. Sparks, C. Vye-Brown, J. Barclay, E. Calder, E. Cottrell, et al. "Global Volcanic Hazards and Risk." In *Global Volcanic Hazards and Risk*, edited by S. C. Loughlin, R.S.J. Sparks, S. K. Brown, S. F. Jenkins, and C. Vye-Brown, 81–173. Cambridge University Press, 2015. https://doi.org/10.1017/CBO9781316276273.004.

Caparros-Martinez, J.L., Milan-Garcia, J., Rueda-Lopez, N., & de Pablo-Valenciano, J. (2020). Green Infrastructure and Water: An Analysis of Global Research. Water, 12(6), 1760. https://doi.org/10.3390/w12061760

CDC Situation Awareness—2022 Volcano Preparedness and Response | CDC Emergency Preparedness & Response. (2022, April 19). https://emergency.cdc.gov/situationawareness/NaturalHazards/Volcano.asp

Constructed Wetlands Manual. (2008). United Nations Human Settlements Programme.

Cook, C. (2016). Regulating the Risks of Domestic Greywater Reuse: A Comparison of England and California. Built Environment (London. 1978), 42(2), 230–242. https://doi.org/10.2148/benv.42.2.230

do Couto, E. de A., Calijuri, M. L., Assemany, P. P., Santiago, A. da F., & Carvalho, I. de C. (2013). Greywater production in airports: Qualitative and quantitative assessment. Resources, Conservation and Recycling, 77, 44–51. https://doi.org/10.1016/j.resconrec.2013.05.004

Eriksson, E., Srigirisetty, S., & Eilersen, A. M. (2010). Organic matter and heavy metals in grey-water sludge. WATER SA, 36(1), 139–142. https://doi.org/10.4314/wsa.v36i1.50921

Farizoglu, B., Nuhoglu, A., Yildiz, E., & Keskinler, B. (2003). The performance of pumice as a filter bed material under rapid filtration conditions. Filtration & Separation, 40(3), 41-+. https://doi.org/10.1016/S0015-1882(03)80137-4

Hafiza, N., Abdillah, A., Islami, B. B., & Priadi, C. R. (2019). Preliminary Analysis of Blackwater and Greywater Characteristics in the Jakarta Greater Region Area. IOP Conference Series: Earth and Environmental Science, 366(1), 012029. https://doi.org/10.1088/1755-1315/366/1/012029

Heins, Pat. Coordinator for Biosolids and Graywater Reuse, Oregon Department of Environmental Quality. Personal communication via virtual interview and email. April 6, 2022.

Heydari, M., Karimyan, K., Darvishmotevalli, M., Karami, A., Vasseghian, Y., Azizi, N., Ghayebzadeh, M., & Moradi, M. (2018). Data for efficiency comparison of raw pumice and manganese-modified pumice for removal phenol from aqueous environments—Application of response surface methodology. Data in Brief, 20, 1942–1954. https://doi.org/10.1016/j.dib.2018.09.027

Houghton, B. F., & Wilson, C. J. (1989). A vesicularity index for pyroclastic deposits. *Bulletin of Volcanology*, *51*(6), 451–462. https://doi.org/10.1007/bf01078811

Kam, S.-K., Kim, J.-K., & Lee, M.-G. (2011). Removal characteristics of mixed gas of ethyl acetate and 2-butanol by a biofilter packed with Jeju scoria. Korean Journal of Chemical Engineering, 28(4), 1019–1022. https://doi.org/10.1007/s11814-010-0480-4

Katukiza, A. Y., Ronteltap, M., Niwagaba, C. B., Kansiime, F., & Lens, P. N. L. (2015). Grey water characterisation and pollutant loads in an urban slum. International Journal of Environmental Science and Technology, 12(2), 423–436. https://doi.org/10.1007/s13762-013-0451-5

Kelm, U., Sanhueza, V., & Guzman, C. (2003). Filtration and retention of mineral processing slurries with pumice and common clay: Low-cost materials for environmental applications in the small-scale mining industry. Applied Clay Science, 24(1–2), 35–42. https://doi.org/10.1016/j.clay.2003.07.004

Khorzughy, S. H., Eslamkish, T., Ardejani, F. D., & Heydartaemeh, M. R. (2015). Cadmium removal from aqueous solutions by pumice and nano-pumice. Korean Journal of Chemical Engineering, 32(1), 88–96. https://doi.org/10.1007/s11814-014-0168-2

Klug, C., Cashman, K. V., & Bacon, C. R. (2002). Structure and physical characteristics of pumice from the climactic eruption of Mount Mazama (Crater Lake), Oregon. Bulletin of Volcanology, 64(7), 486–501. https://doi.org/10.1007/s00445-002-0230-5

Kuslu, Y., & Sahin, U. (2013). A comparison study on the removal of suspended solids from irrigation water with pumice and sand-gravel media filters in the laboratory scale. Desalination and Water Treatment, 51(10–12), 2047–2054. https://doi.org/10.1080/19443994.2013.734492

Laaffat, J., Aziz, F., Ouazzani, N., & Mandi, L. (2019). Biotechnological approach of greywater treatment and reuse for landscape irrigation in small communities. Saudi Journal of Biological Sciences, 26(1), 83–90. https://doi.org/10.1016/j.sjbs.2017.01.006

Li, R., Zhang, Y., Chu, W., Deng, Z., Chen, Z., & Tian, D. (2021). Natural Mineral for Remediation of Iron- and Manganese-Contaminated Groundwaters. Polish Journal of Environmental Studies, 30(3), 2161–2171. https://doi.org/10.15244/pjoes/98996

Lisowski, Michael, Robert McCaffrey, Charles W. Wicks, and Daniel Dzurisin. "Geodetic Constraints on a 25-year Magmatic Inflation Episode Near Three Sisters, Central Oregon." *Journal of Geophysical Research: Solid Earth* 126, no. 12 (December 2021). https://doi.org/10.1029/2021JB022360.

Misra, R. K., Patel, J. H., & Baxi, V. R. (2010). Reuse potential of laundry greywater for irrigation based on growth, water and nutrient use of tomato. Journal of Hydrology, 386(1–4), 95–102. https://doi.org/10.1016/j.jhydrol.2010.03.010

Mueller, S., Scheu, B., Kueppers, U., Spieler, O., Richard, D., & Dingwell, D. B. (2011). The porosity of pyroclasts as an indicator of volcanic explosivity. *Journal of Volcanology and Geothermal Research*, *203*(3), 168–174. https://doi.org/10.1016/j.jvolgeores.2011.04.006

Myers, Bobbie, and Carolyn Driedger. "Eruptions in the Cascade Range During the Past 4,000 Years," 2008. https://pubs.usgs.gov/gip/63/.

Nelson, M. (2014). The wastewater gardener: Preserving the planet one flush at a time! (First edition.). Synergetic Press.

Oregon History Project. (n.d.). https://www.oregonhistoryproject.org/narratives/central-oregon-adaptation-and-compromise-in-an-arid-landscape/finding-central-oregon/prehistory/#.YLuB65NKhpQ.

Oteng-Peprah, M., Acheampong, M. A., & deVries, N. K. (2018). Greywater Characteristics, Treatment Systems, Reuse Strategies and User Perception-a Review. Water Air and Soil Pollution, 229(8), 255. https://doi.org/10.1007/s11270-018-3909-8

Oteng-Peprah, M., de Vries, N. K., & Acheampong, M. A. (2018). Greywater characterization and generation rates in a pen urban municipality of a developing country. Journal of Environmental Management, 206, 498–506. https://doi.org/10.1016/j.jenvman.2017.10.068

Pinto, G. O., Soares da Silva Junior, L. C., Nagem Assad, D. B., Pereira, S. H., & Brasil de Brito Mello, L. C. (2021). Trends in global greywater reuse: A bibliometric analysis. Water Science and Technology, 84(10–11), 3257–3276. https://doi.org/10.2166/wst.2021.429

Shea, T., Houghton, B. F., Gurioli, L., Cashman, K. V., Hammer, J. E., & Hobden, B. J. (2010). Textural studies of vesicles in volcanic rocks: An integrated methodology. Journal of Volcanology and Geothermal Research, 190(3), 271–289. https://doi.org/10.1016/j.jvolgeores.2009.12.003

Trafton, K.R. and Giachetti, T., 2021. The morphology and texture of Plinian pyroclasts reflect their lateral sourcing in the conduit. *Earth and Planetary Science Letters*, *562*, p.116844.

Water Research Centre (WRC). (n.d.). *Water and wastewater treatment*. Water and Wastewater Treatment . Retrieved March 8, 2022, from https://www.wrc.unsw.edu.au/abc-staff

Welcome. Whose Land. (n.d.). https://www.whose.land/en/.

Wiejaczka, J. and Giachetti, T., 2022. Using Eruption Source Parameters and High-Resolution Grain-Size Distributions of the 7.7 ka Cleetwood Eruption of Mount Mazama (Oregon, United States) to Reveal Primary and Secondary Eruptive Processes. *Frontiers in Earth Science*, p.460.